NAVAL POSTGRADUATE SCHOOL
Monterey, California

THESIS

THE INFLUENCE OF TOTAL STRAIN,
STRAIN RATE AND REHEATING TIME DURING
WARM ROLLING ON THE SUPERPLASTIC DUCTILITY
OF AN AL-MG-ZR ALLOY

by

James E. Wise II

March 1987

Thesis Advisor: T. R. McNelley

SECURITY CLASSIFICATION OF THIS PAGE

REPORT DOCUMENTATION PAGE

1a REPORT SECURITY CLASSIFICATION UNCLASSIFIED	1b RESTRICTIVE MARKINGS
2a SECURITY CLASSIFICATION AUTHORITY	3 DISTRIBUTION/AVAILABILITY OF REPORT Approved for public release; distribution is unlimited.
2b DECLASSIFICATION/DOWNGRADING SCHEDULE	
4 PERFORMING ORGANIZATION REPORT NUMBER(S)	5 MONITORING ORGANIZATION REPORT NUMBER(S)
6a NAME OF PERFORMING ORGANIZATION Naval Postgraduate School 6b OFFICE SYMBOL (If applicable) 69	7a NAME OF MONITORING ORGANIZATION Naval Postgraduate School
6c ADDRESS (City, State, and ZIP Code) Monterey, California 93943-5000	7b ADDRESS (City, State, and ZIP Code) Monterey, California 93943-5000
8a NAME OF FUNDING/SPONSORING ORGANIZATION 8b OFFICE SYMBOL (If applicable)	9 PROCUREMENT INSTRUMENT IDENTIFICATION NUMBER
8c ADDRESS (City, State, and ZIP Code)	10 SOURCE OF FUNDING NUMBERS PROGRAM ELEMENT NO / PROJECT NO / TASK NO / WORK UNIT ACCESSION NO

11 TITLE (Include Security Classification)
THE INFLUENCE OF TOTAL STRAIN, STRAIN RATE AND REHEATING TIME DURING WARM ROLLING ON THE SUPERPLASTIC DUCTILITY OF AN AL-MG-ZR ALLOY

12 PERSONAL AUTHOR(S)
Wise, James E.

13a TYPE OF REPORT	13b TIME COVERED FROM ____ TO ____	14 DATE OF REPORT (Year, Month Day)	15 PAGE COUNT
Master's Thesis		1987, March	83

16 SUPPLEMENTARY NOTATION

17 COSATI CODES			18 SUBJECT TERMS (Continue on reverse if necessary and identify by block number)
FIELD	GROUP	SUB-GROUP	Superplastic, Ductility, Total strain, Strain rate, Reheat Time, Continuous recrystallization

19 ABSTRACT (Continue on reverse if necessary and identify by block number)

The effect of varying three processing variables on the superplastic ductility of an Al-10Mg-0.1Zr alloy was studied. The three variables investigated were: (1) time at temperature during warm rolling; (2) strain rate during rolling (by varying reduction per pass); and (3) total strain. After the material was warm rolled, samples were tension tested at 300°C and at strain rates varying from $6.67 \times 10^{-5} S^{-1}$ to $1.67 \times 10^{-1} S^{-1}$. The greatest superplastic ductilities were achieved in material experiencing the largest total strain, lowest strain rate and most prolonged reheating time during warm rolling. The results are consistent with a model for structure development based on continuous recrystallization.

20 DISTRIBUTION/AVAILABILITY OF ABSTRACT	21 ABSTRACT SECURITY CLASSIFICATION	
☒ UNCLASSIFIED/UNLIMITED ☐ SAME AS RPT ☐ DTIC USERS	UNCLASSIFIED	
22a NAME OF RESPONSIBLE INDIVIDUAL T. R. McNelley	22b TELEPHONE (Include Area Code) (408) 646-2589	22c OFFICE SYMBOL 69Mc

DD FORM 1473, 84 MAR 83 APR edition may be used until exhausted
All other editions are obsolete

SECURITY CLASSIFICATION OF THIS PAGE

Approved for public release; distribution is unlimited.

The Influence of Total Strain, Strain Rate and Reheating Time During Warm Rolling on the Superplastic Ductility of an Al-Mg-Zr Alloy

by

James E. Wise II
Lieutenant, United States Navy
B.S., U.S. Naval Academy, 1979

Submitted in partial fulfillment of the requirements for the degree of

MASTER OF SCIENCE IN MECHANICAL ENGINEERING

from the

NAVAL POSTGRADUATE SCHOOL
March 1987

ABSTRACT

The effect of varying three processing variables on the superplastic ductility of an Al-10Mg-0.1Zr alloy was studied. The three variables investigated were: (1) time at temperature during warm rolling; (2) strain rate during rolling (by varying reduction per pass); and (3) total strain. After the material was warm rolled, samples were tension tested at 300 C and at strain rates varying from 6.67×10^{-5} S^{-1} to 1.67×10^{-1} S^{-1}. The greatest superplastic ductilities were achieved in material experiencing the largest total strain, lowest strain rate and most prolonged reheating time during warm rolling. The results are consistent with a model for structure development based on continuous recrystallization.

TABLE OF CONTENTS

LIST OF TABLES

LIST OF FIGURES

ACKNOWLEDGEMENT

I would like to thank my advisor, Professor T.R. McNelley and Dr. S. J. Hales for their expert assistance in conducting this research. Also my sincere thanks to T. Kellogg and Tamara Bloomer whose technical expertise and material support was essential to me during the experimental phase of this thesis. Additionally, I would like to thank my friends and co-workers, A. Salama, B. Sanchez, D. Solomos, and D. Stewart for their insight which added depth to my thesis. Finally, I would like to express my deepest thanks to my wife Pamela for her support during my tour of duty at NPS.

I. INTRODUCTION

Superplastic behavior has been reported in many different alloys and even in ceramics [Ref. 1] and the common denominators in all cases are first, a fine grain size (on the order of 1-10 um); second, deformation at temperatures >0.5 Tm; and third, a strain rate sensitivity coefficient m>0.3. The strain rate range associated with superplastic behavior increases with decreasing grain size and increasing temperature [Ref. 1]. The interest in superplastic behavior has increased over the years because of the new opportunities for application these materials offer. These opportunities include ability to form complex shapes in one piece, elimination of fasteners and welds in high strength components with complex geometries and production in one piece of structural components requiring a combination of good ductility and toughness, high strength and light weight [Ref. 2]. It is generally accepted that before a material is considered to be superplastic, elongations to failure of at least two hundred percent must be attained; here, elogations up to 400 percent have been attained.

Research over the past seven years at the Naval Postgraduate School has concentrated on high Magnesium, Aluminum-Magnesium alloys. High-Mg alloys were studied at NPS because of their moderate to high strength, good

ductility, low density, good toughness, corrosion resistance (when processed correctly) and good high cycle fatigue behavior [Ref. 3]. Furthermore, Magnesium is highly soluble in Aluminum (see Figure 1.1) and thus contributes to strengthening by solid solution strengthening [Ref. 2]. Early research by Johnson and Sirah [Refs. 4,5] at NPS on high-Mg, Al-Mg alloys has developed a thermomechanical process (TMP) that includes: (1) solution treatment above the solvus to dissolve all soluble components; (2) hot working by upset forging to further refine and homogenize the microstructure; (3) oil quenching from solution treatment to provide a metastable structure [Ref. 6]; and (4) reheating in conjunction with warm working to large strains at a temperature below the Mg-solvus. This increases the ambient temperature strength of the material through a combination of dislocation substructure, dispersion and solid solution strengthening by providing a fine dispersion of the beta phase (Mg_5Al_8) in a solid solution matrix also containing a refined dislocation structure [Ref. 3]. The focus of this study is to enhance understanding of the thermomechanical process (TMP) by conducting a study where three process variables are varied: (1) the total strain during the warm rolling; (2) rate of straining by varying the reduction per pass; and (3) the reheating time during warm rolling. The effects of these variables on the superplastic behavior of this material will be studied and documented.

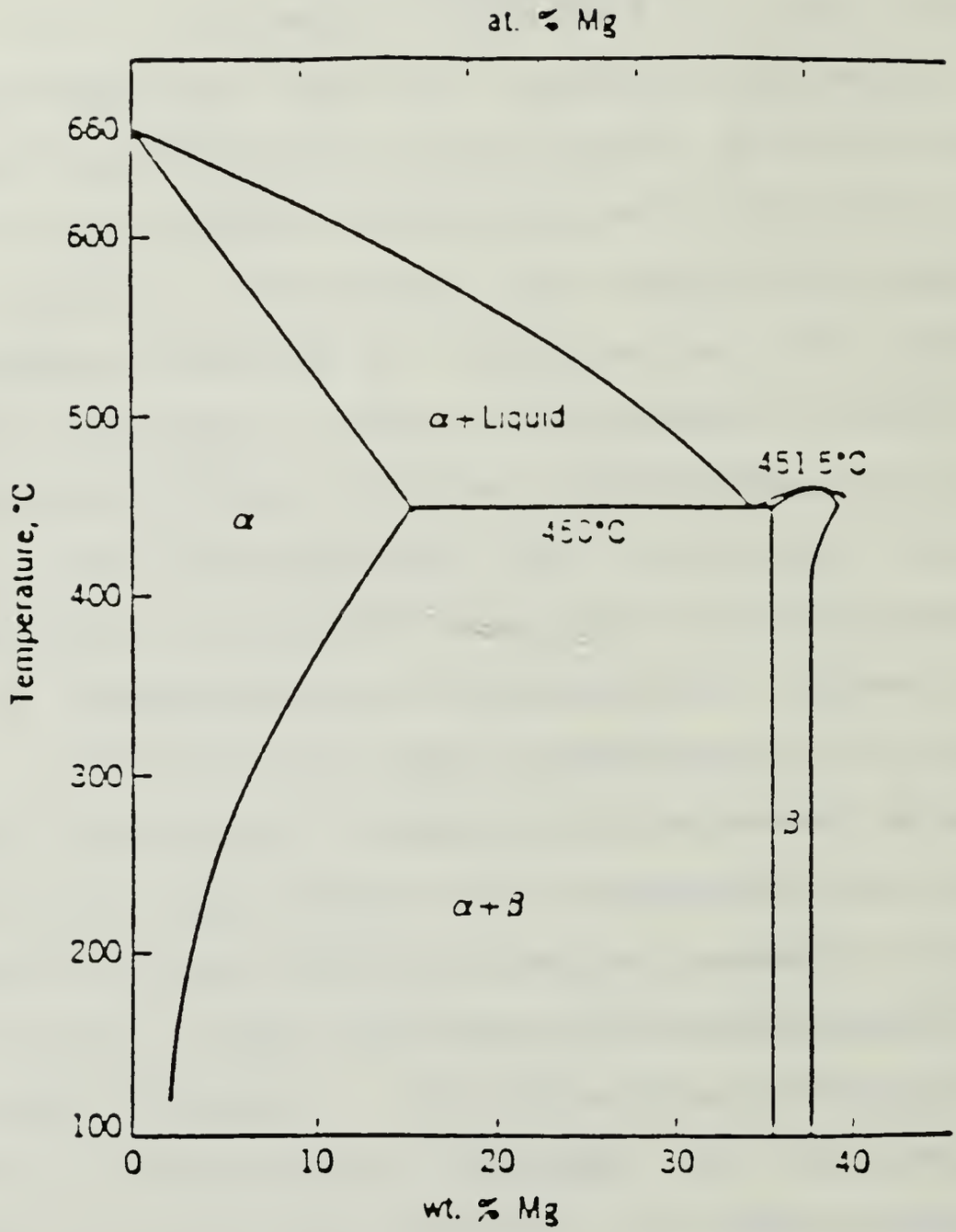

Figure 1.1 Partial Aluminum-Magnesium Phase Diagram.

Data for this thesis was obtained from mechanical testing of the as-rolled material as well as from microstructal examination using the scanning electron microscope and optical microscopy. Finally, new questions are posed for subsequent research.

II. BACKGROUND

A. ALUMINUM-MAGNESIUM ALLOYS

Aluminum alloys are preferred in many aerospace and other military applications because of their potentially high strength-to-weight ratio, corrosion resistance, and good toughness and ductility. The most common alloying elements used are Copper, Manganese, Silicon, Magnesium, and Zinc. In the Aluminum-Magnesium system, increased strength is obtained primarily through solid solution strengthening and work hardening. Any beta phase (Al_8Mg_5) should be fine and uniformly distributed throughout the parent phase. The maximum solubility of Magnesium in Alumininum is about 15 percent at the eutectic temperature of 451 C (see Figure 1.1). The beta is a hard inter-metallic compound. Problems arise in alloys with high Magnesium concentration because the beta tends to precipitate along the grain boundaries. This creates a Magnesium-depleted zone near the grain boundaries, resulting in the material becoming susceptible to intergranular corrosion and stress-corrosion cracking [Ref. 7]. It has been found that at concentrations approaching 15 percent Magnesium, the alloy becomes too brittle at ambient temperature for structural applications. Most commercial Al-Mg alloys contain less than six percent Mg; in this work, alloys containing 10 percent Mg were

studied. This provides sufficient Mg such that the interaction between Mg precipitation and deformation can be studied but not so much that ambient temperature properties are degraded.

B. TERNARY ADDITIONS

The addition of Zirconium was done to control grain growth through very fine $ZrAl_3$ dispersoids without affecting the Mg-solubility. This would allow increased microstructural stability during superplastic forming [Ref. 3].

C. SUPERPLASTIC BEHAVIOR

Although superplastic behavior has been observed in many alloy systems over the years, it was not actively studied in the U.S. until Underwood [Ref. 8] published the first English language review in 1962. Since then a considerable effort has been directed at this phenomenon. The most commonly accepted characteristics of a superplastic material are: (1) a fine, equiaxed grain structure with high angle boundaries; (2) a deformable second phase if present; (3) low strain rates; (4) elevated temperatures equal to 0.5-0.7 Tm; (5) resistance to cavitation; and (6) a thermally stable structure [Ref. 9].

Two primary approaches exist when analyzing superplastic behavior. They are first, the material science approach which through microstructural analysis, attempts to understand superplasticity; and secondly, through applied

mechanics that explains the phenomenon in terms of strain rate sensitivity of the material.

1. Strain Rate Sensitivity

Superplastic deformation is a thermally activitated process which is only observed at elevated temperatures. In analysis of deformation, a power law relation, Equation 2.1, is used to relate the flow stress (σ) and the strain rate ($\dot{\varepsilon}$):

$$\sigma = k\dot{\varepsilon}^{m} \qquad \text{(eqn. 2.1)}$$

where k is a material constant and m is the strain rate sensitivity coefficient. The "m" value can be calculated by using Equation 2.2 below:

$$m = \frac{d(\ln\sigma)}{d(\ln\dot{\varepsilon})} \qquad \text{(eqn. 2.2)}$$

or by evaluating the slope of the log stress versus log strain rate data from experiment as in Chapter IV of this thesis. Typical superplastic materials have an "m" value that ranges from 0.3-0.7 with an "m" value of 1.0 being a Newtonian fluid. Hart [Ref. 10] revealed that a high resistance to localize necking is observed in materials that are highly strain rate sensitive and most superplastic metals have $m \simeq 0.5$ [Ref. 2].

2. Deformation Mechanisms

Several theories have been proposed to account for deformation at elevated temperature. At high temperatures

and low stresses, where the creep strain rate varies linearly with the applied stress, Nabarro [Ref. 11] and Herring [Ref. 12] postulated that creep occurred by a stress-directed diffusional process. This "diffusional creep" involves the migration of vacancies along a gradient between boundaries that are in tension to boundaries that are experiencing compression. Simultaneously, atoms would be moving in the opposite direction causing an elongation of the grains. This Nabarro-Herring creep model is described below by Equation 2.3:

$$\dot{\varepsilon}_s \simeq \frac{7\sigma D_v b^3}{kTd^2} \qquad \text{(eqn. 2.3)}$$

where $\dot{\varepsilon}$ is the steady state creep rate, b is the Burger's vector, D_v is the volume diffusivity, T is absolute temperature, k is Boltzmann's constant, d is the grain size and σ is the applied stress.

A similar theory proposed by Coble [Ref. 13] involves atomic diffusion along grain boundaries. The Coble creep relationship is described below by Equation 2.4:

$$\dot{\varepsilon}_s = \frac{50\sigma D_b b^4}{kTd^3} \qquad \text{(eqn. 2.4)}$$

where D_b is the boundary diffusivity. Note that the Coble creep model is more sensitive to grain size than the Narbarro-Herring model [Ref. 1].

Further studies conducted by Ashby [Ref. 14] combined both the Nabarro-Herring and Coble creep model into the following equation:

$$\dot{\varepsilon} \simeq \frac{14\sigma b^3 D_v}{kTd^2} \frac{(1+\pi\delta D_b)}{(dD_v)} \qquad \text{(eqn. 2.5)}$$

where D_v is volume diffusivity, D_b is boundary diffusivity and δ is grain boundary thickness. All other variables are as described before. This model shows that both boundary and volume diffusion will contribute to straining in an additive sense with both processes competing with each other, the faster process being the one observed. [Ref. 15]

Ashby and Verrall [Ref. 16] postulated a mechanism for producing the larger strains encountered in superplastic materials. This model involves grain boundary sliding accomodated by duffusion (see Figure 2.1). The Ashby-Verrall investigation resulted in the model described below by Equation 2.6.

$$\dot{\varepsilon} = \frac{98 b^3 D_v}{kTd^2} \frac{(\sigma - 0.72\Gamma)}{(d)} \frac{1+\pi\delta D_b}{dD_v} \qquad \text{(eqn. 2.6)}$$

where Γ is the grain boundary surface energy and all other terms are described as before.

The Ashby-Verrall model is similar to the Narbarro-Herring and Coble models in that all predict an inverse grain size dependance. Conversely, the models differ in a

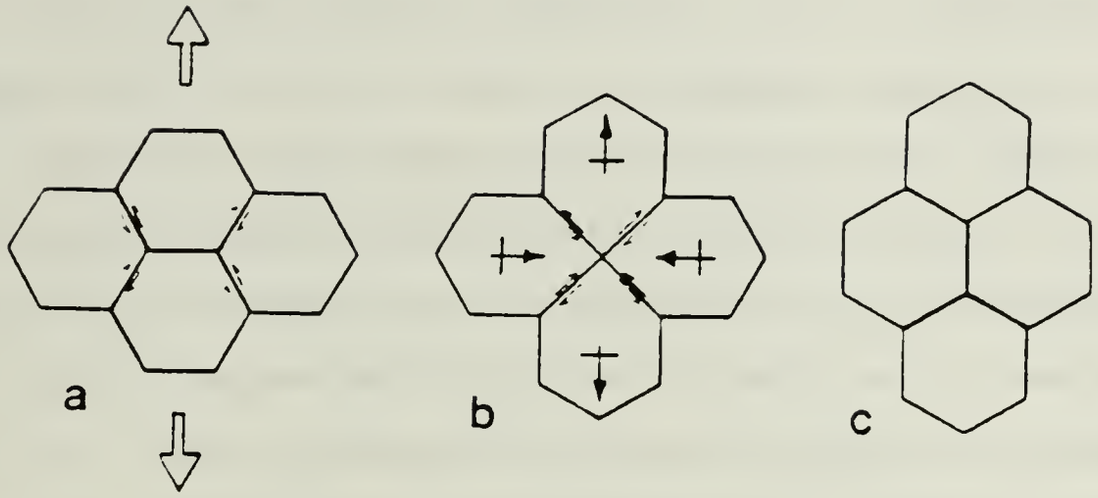

Figure 2.1 Ashby-Verrall Grain Boundary Sliding Model.

topological sense because grain exchange locations with their neighbors as seen in Figure 2.1 and do not elongate significantly.

Sherby and Wodsworth [Ref. 17] propose a phenomenological model, predicting the grain size effect on superplastic flow, and given below as:

$$\dot{\varepsilon} = \frac{KD^{*}_{eff}}{d^{p}} \left(\frac{\sigma^{m}}{E} \right) \qquad \text{(eqn. 2.7)}$$

where $\dot{\varepsilon}$ is the strain rate, p is the grain size exponent, D^{*}_{eff} is the effective diffusion coefficient and k is the material constant. The above equation shows that for a constant strain rate as the grain size increases, the stress required for deformation will also increase. Grain growth during deformation would result in a "strain hardening" effect. Increased grain size results in greater diffusion

distances; this in turn causes a diffusion flux to decrease for a given strength and the result is an apparently stronger, more creep-resistant material. [Ref. 18]

Zener and McLean theorized that grain boundaries of growing grains would interact with dispersed particles and become pinned due to a retarding force arising from boundary-particle interaction balancing with the driving force caused by the reduction in surface energy of the grains. The Zener-McLean relationship is described below:

$$d=\frac{4r}{3f} \qquad \text{(eqn. 2.8)}$$

where d is grain size, f is volume fraction of particles, and r is particle radius. Equation 2.8 clearly illustrates that for a given volume fraction of precipitate, a smaller particle radius will result in a finer grain size. [Ref. 2]

D. THERMOMECHANICAL PROCESS (TMP)

Thermomechanical processing of Aluminum alloys has been extensively reviewed by Williams [Ref. 19], McQueen [Ref. 20] and McQueen et al. [Ref. 21]. Several thermomechanical treatments have been done in which the interplay of precipitates or constiuent particles with deformation to refine grain size, enhance strength, toughness and improved ductility were utilized. The benefits gained by manipulating Zirconium, Manganese Chromium additions, combined with the appropriate thermomechanical process, led

to grain size control which is a requirement for superplastic behavior. [Ref. 22] Previous work NPS with 8-10% Al-Mg alloys by Johnson and Sirah [Refs. 4, 5] resulted in a thermomechanical process that enhanced stress-corrosion resistance, improved fatigue resistance, increased ductility and improved elevated and ambient properties. The purpose of this thesis is to carry on the research that Alcamo, Berthold, Hartmann and Grider [Refs. 7, 2, 15, 3] did in an attempt to study the effects of the Zirconium addition to high Magnesium alloys. This research will concentrate on the warm-rolling phase of the (TMP) and study its effect on the superplastic response of both the Al-10Mg and Al-10Mg-0.1Zr alloys, by varying total strain, straining rate and reheating time between each rolling pass during the TMP. These results will be correlated with the anticipated effect of these variables on the microstructure.

III. EXPERIMENTAL PROCEDURE

A. MATERIAL

The two aluminum alloys studied in this research contained nominally 10% Mg; one alloy contained 0.1% Zr in addition, and the second alloy contained 10% Mg only. The ingots used in this research were produced by ALCOA Technical Center. The ingots were direct-chill cast using 99.99% pure aluminum base metal alloyed with commercially pure magnesium, Al-Zr master alloy, with a Ti-B addition for grain size control in the as-cast condition, and Beryllium as 5% Be Aluminum-Beryllium master alloy for oxidation control [Ref. 23]. The as-received ingots, serial numbers S572826 and S572824, were approximately 1016mm (44 in) in length and 127mm (5 in) in diameter. The complete chemical composition is listed in Table I. [Ref. 23]

TABLE 1
ALLOY COMPOSITION (WEIGHT PERCENT)

Serial Number	Mg	Zr	Si	Fe	Ti	Be	Pb	Al
S572826	9.89	0.09	0.02	0.02	0.01	0.0003	-	Bal.
S572824	10.05	0.01	0.01	0.02	0.01	0.0003	0.01	Bal.

B. PROCESSING

The ingots were sectioned into billets 95.3 mm (3.75 in) long with a cross section 31.8mm (1.25 in) square. These billets were initially solution treated above the solvus at 440° C for 5 hours and then at 480°C for 19 hours using the

procedure developed by Johnson [Ref. 4] and refined by Becker [Ref. 24]. The temperature was monitored using two thermocouples. After solution treating, the billets were upset forged longitudinally at 480°C on heated platens to approximately 25.4mm (1 in) in height. However, during the upset forging stage, cracking of some of the billets occurred. This likely was caused by liquation of grain boundaries resulting in intergranular fracture. This phenomenon is further documented in Chapter IV. To alleviate the cracking, solution treatment was done at 440°C for 40 hours as illustrated in Figure 3.1; time was extended to offset reduced temperature. After upset forging, the billets were resolution treated for 1 hour at 440°C and then vigorously oil quenched. This hot working resulted in a reduction of approximately 71% and for a true strain of 1.3.

C. WARM ROLLING

Each billet was then warm rolled within 24 hours as described by Grider [Ref. 3]. All billets were heated at 300° C to achieve isothermal conditions prior to the first rolling pass. A total of 5 different processes were achieved by varying the percentage reduction per pass, the interpass reheating time and total true final strain. These processing variables are illustrated in Figure 3.1 and the schedules used are also described in Table II below.

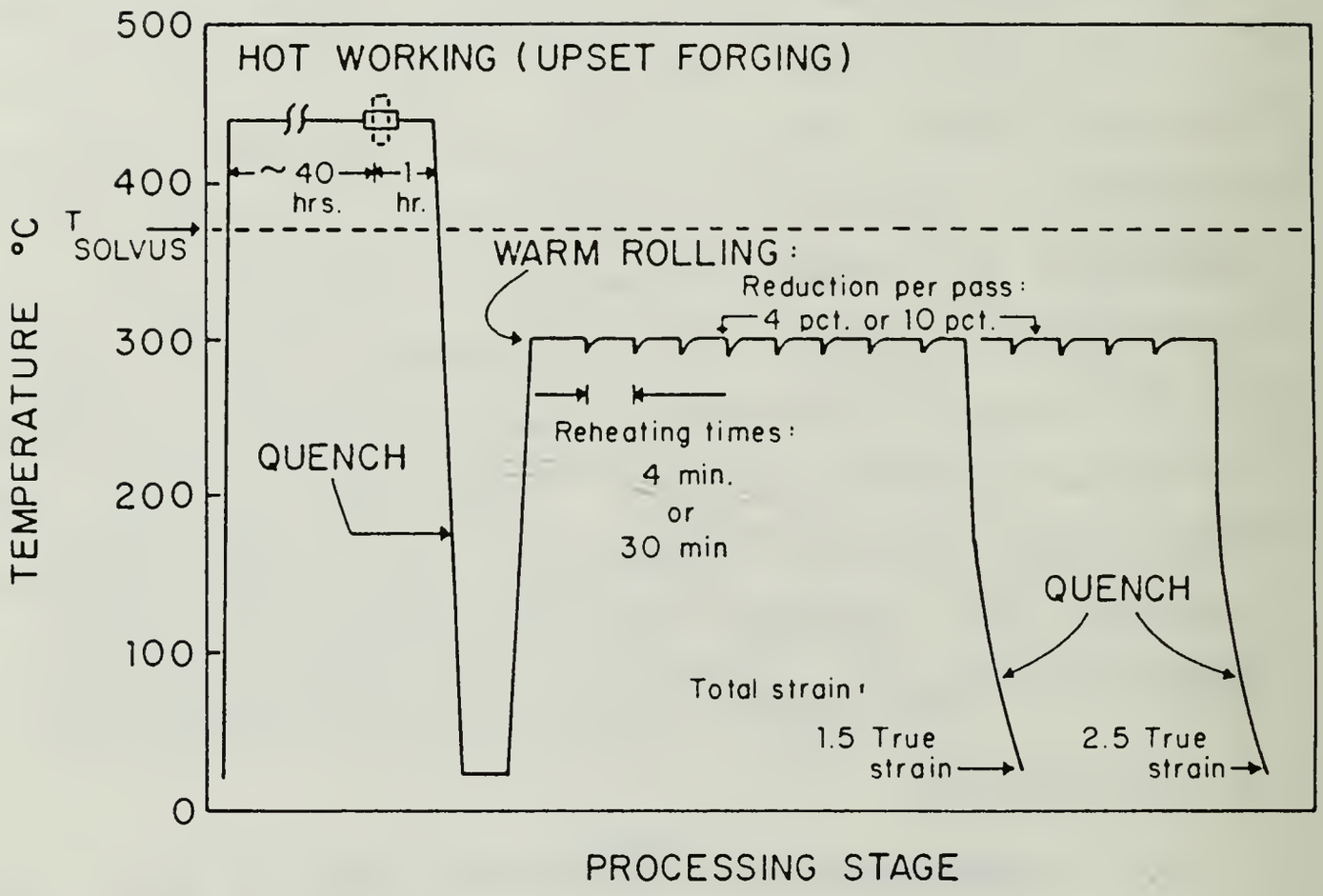

Figure 3.1 Thermomechanical Processing Technique.

TABLE II
PROCESSING SCHEDULES

	Processes				
	A	B	C	D	E
Pct. Red. Per Pass	10	4	4	10	4
Reheating Time Between Passes	4	4	30	4	4
Total True Strain	2.5	2.5	2.5	1.5	1.5

From the above table, 10 percent reduction per pass will be referred as the heavy reduction schedule and the 4 percent reduction will be referred as the light reduction schedule. The warm rolling processes are lettered from A to E progressing from the most severe heavy reduction schedule to the least severe light reduction schedule. The hot working and warm working were done in the region of Al-Mg phase diagram illustrated in Figure 3.2. [Ref. 18]

D. SPECIMEN FABRICATION

Specimen fabrication was accomplished in accordance with procedure established by Becker [Ref. 24] and Hartmann [Ref. 15]. After warm rolling, final sheet reduction was approximately 80% for schedules D and E, resulting in a sheet thickness of approximately 0.18 inches; and approximately 93% for schedules A-C, with a sheet thickness of approximately .075 inches. Depending on actual thickness and end wastage, 7 to 25 specimens could be fabricated from each sheet in accordance with specimen geometry shown in

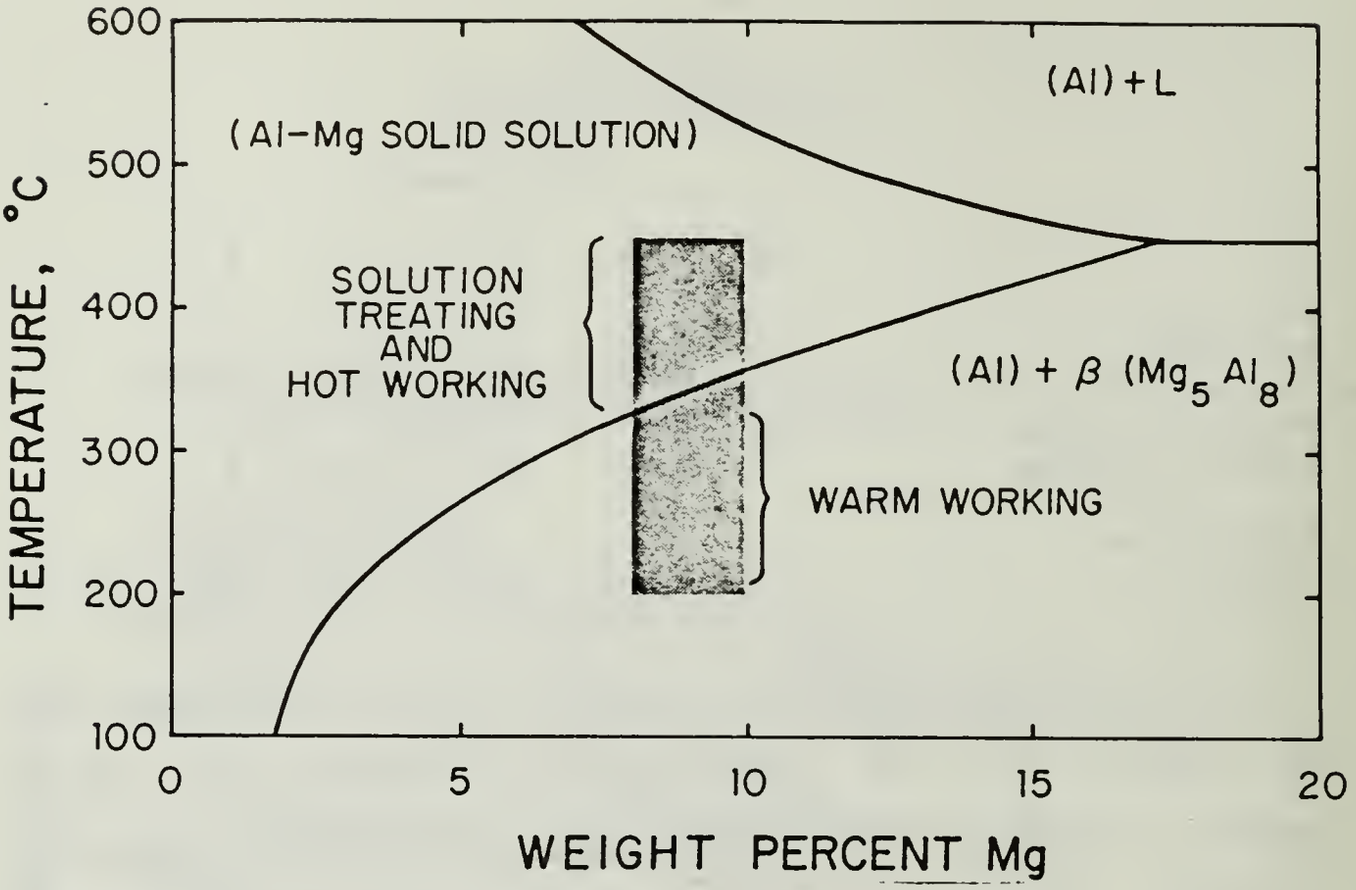

Figure 3.2 Portion of the Al-Mg Phase Diagram Showing Where Material Processing Was Done.

Figure 3.3. This test specimen geometry was an improved design that effectively distributed the gripping forces of the wedges over the whole tab area of the specimen. This design also made it easier to determine the gage section of the specimen.

E. MECHANICAL TESTING

Mechanical testing was done following procedures outlined by Becker [Ref. 24] and Hartmann [Ref. 15], with minor modifications. Elevated temperature testing was conducted using an electromechanical Instron machine. Before each series of tests the Instron machine was calibrated. Specimens were mounted in wedge-type grips

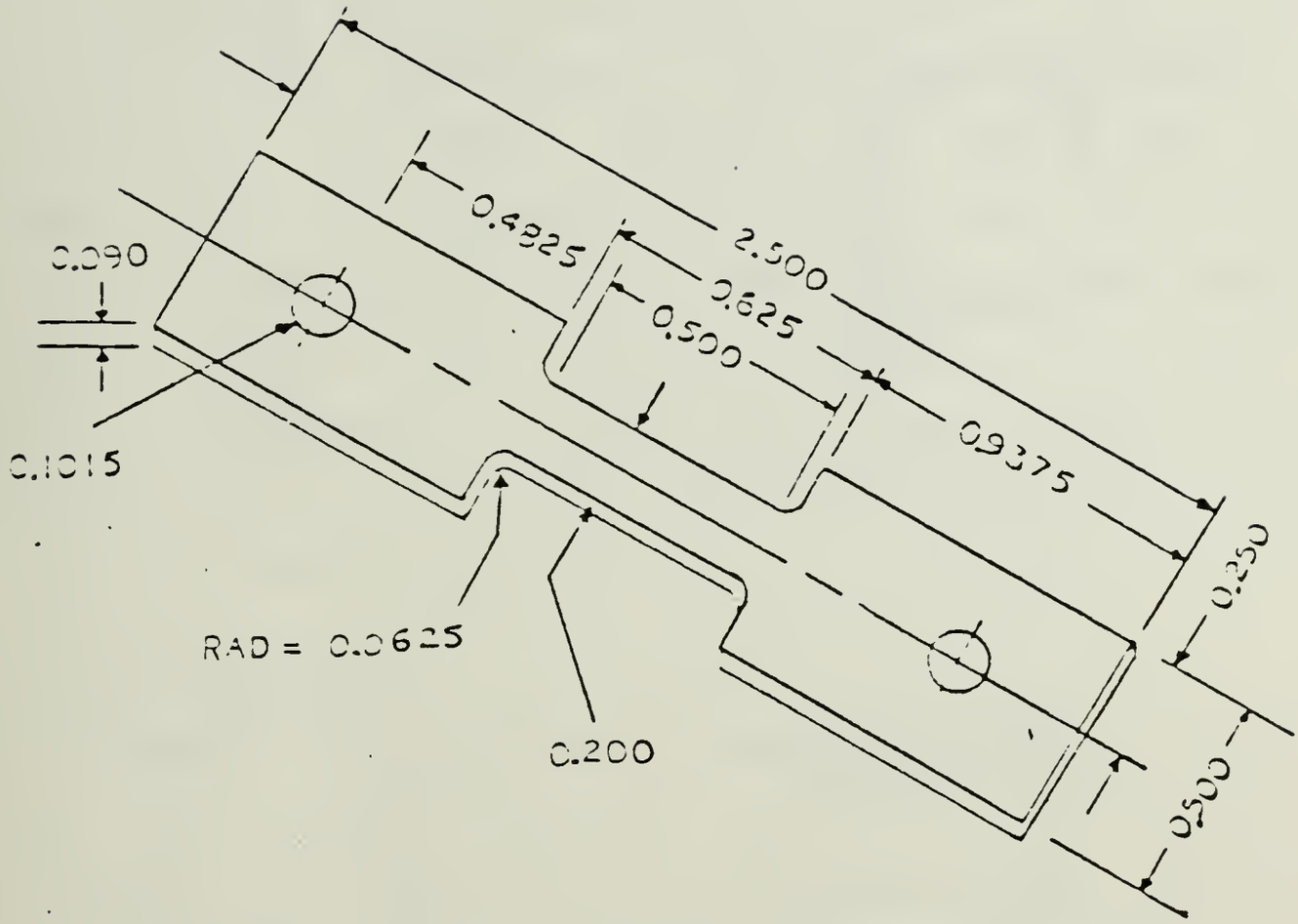

Figure 3.3 Tensile Test Specimen Geometry.

supplied by ATS, Butler, Pennsylvania and fabricated using Inconel 718 for elevated temperature testing. A Marshall Model 2232 three-zone clamshell furnace mounted on the Instron was used to conduct elevated temperature testing at 300° C. The furnace temperature was maintained by three separate controllers, which controlled 3 vertically-oriented heating elements. Insulation and sheathed thermocouple placement was done similar to the procedure outlined by Hartmann [Ref. 15] with the exception that four

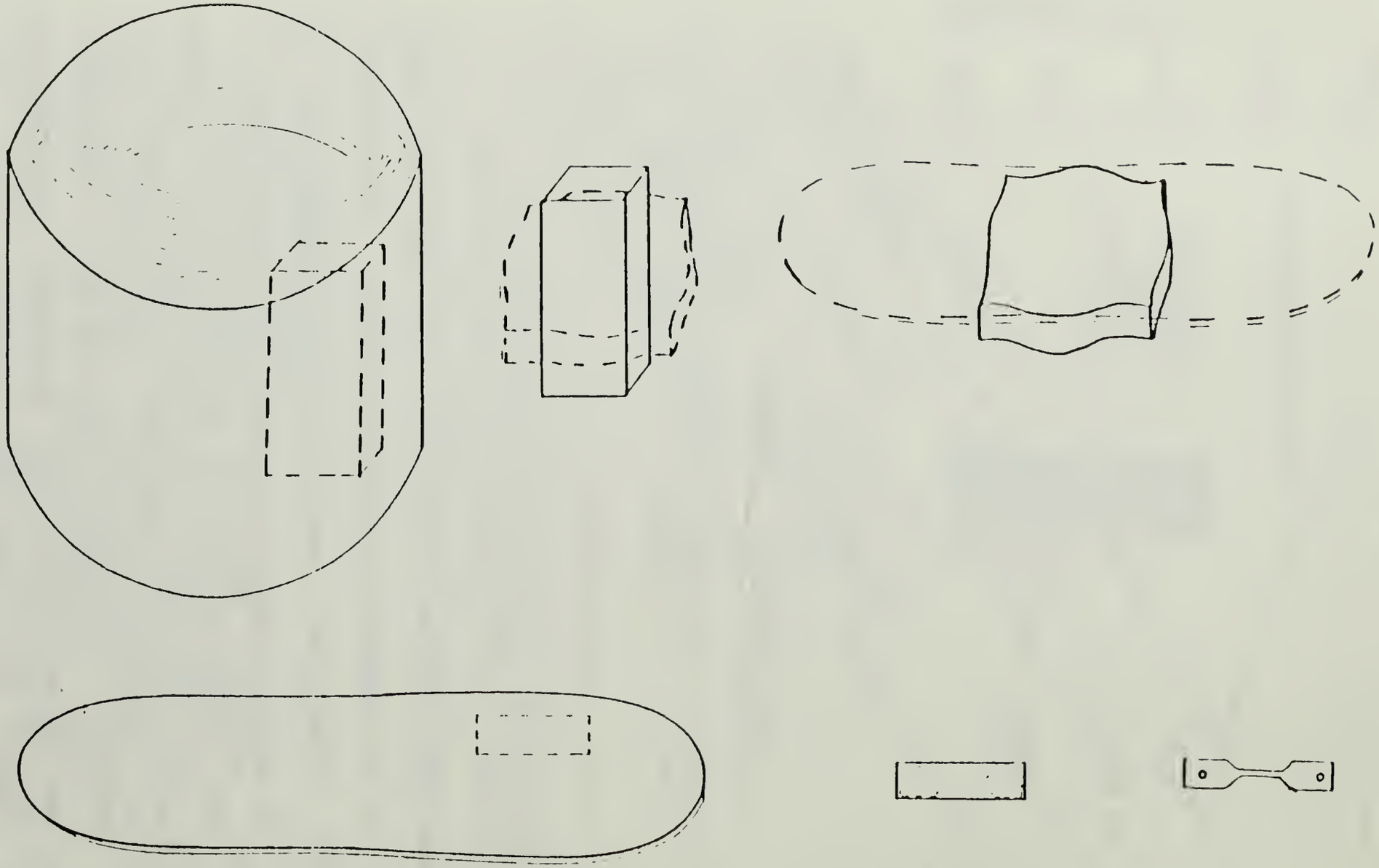

Figure 3.4 Evolution of Tensile Test Specimens.

thermocouples were used instead of five. Accurate temperature readings were still achieved with four thermocouples within +/- one degree centigrade. It would normally take approximately 90 minutes for the clamshell furnace to reach 300°C. After the first tensile test of each series was conducted, it would only take 30 to 40 minutes to stabilize at 300°C. The crosshead speeds ranged from 0.05mm/min (.002 in/min) to 127mm/min (5.0 in/min) which corresponded to nominal strain rates varying from $6.67 \times 10^{-5}\ S^{-1}$ to $1.67 \times 10^{-1}\ S^{-1}$. Specimens tested were in the as-rolled condition [Ref. 3].

F. DATA REDUCTION

Elongation was determined by measuring the gauge length prior to fracture and again after fracture. Percent elongation was determined by taking the difference between the initial and final gauge lengths, dividing by the initial gauge length and then multiplied by 100. The Instron strip chart measured applied load (lbs.) verses displacement. A "floating slope" was used to take raw data from the strip chart. This "floating slope" made corrections for such variables as grip slippage, elasticity of sample and the Instron components themselves [Ref. 3]. The magnification ratios used for data reduction were 10, 40 and 100. The smaller ratio was for strain rates $10^{-3}\ S^{-1}$ or greater and the higher ratios were used for the strain rates less than $10^{-3}\ S^{-1}$. All raw data was analyzed using a Basic computer

program developed by Grider [Ref. 3]. A copy of this program is included in Appendix B. All reduced data was graphically presented using EASYPLOT.

G. OPTICAL MICROSCOPY

The ZEISS ICM 405 optical microscope was used to examine specimens in the as-rolled condition. Transverse and longitudinal micrographs were taken of the samples and are explained in further detail in Chapter IV. The samples were prepared using the process developed by Oster [Ref. 25] and Grider [Ref. 3].

H. SCANNING ELECTRON MICROSCOPY (SEM)

A CAMBRIDGE STEREOSCAN 200 scanning electron microscope was used to examine the fracture surface and fracture tip of the specimens that exhibited the highest ductility for processes A, B and C, subsequently deformed at strain rates of $1.67 \times 10^{-3}\ S^{-1}$, $6.67 \times 10^{-3}\ S^{-1}$ and $6.67 \times 10^{-4}\ S^{-1}$. These specimens were prepared by cleansing the fracture surface with ethyl alcohol and then air drying. Micrographs of these specimens are included in Chapter IV.

IV. RESULTS AND DISCUSSION

This chapter reports the results obtained in this research and compares data with previous studies done at NPS, specifically those of Alcamo [Ref. 7] and Grider [Ref. 3]. The thermomechanical process itself was studied here: the total strain, the straining rate and the reheating time between each rolling pass were the the variables investigated. This was accomplished by obtaining mechanical test data on materials processed in different ways and then comparing the processes as described in Table II. Also, microscopy was done using both optical and scanning electron microscopy.

A. MECHANICAL TESTING RESULTS

Mechanical testing was done to study the deformation properties of processes A thru E. As described in Chapter III, tensile testing was done at 300°C with strain rates varying from 6.67×10^{-5} S^{-1} to 1.67×10^{-1} S^{-5} as shown in Tables III and IV. A graphical representation for a series of tension tests on as-rolled material using process C are provided in Figure 4.1. Stress-strain curves for the other processes are shown in Appendix A. After the maximum stress value is reached, the true strain-true stress value is suspect due to the onset of necking. These curves exhibit prolonged necking during deformation which is a common trait of superplastic materials [Ref. 3].

TABLE III

DATA FOR Al-10%Mg-0.1%Zr ALLOY IN THE AS-ROLLED CONDITION

Process	Temperature °C	Strain Rate S^{-1}	True Strain at 0.1 Plastic Strain (PSI)	Ductility %
A	300	6.67×10^{-5}	3500	258
	300	1.67×10^{-4}	3750	190
	300	6.67×10^{-4}	4700	213
	300	1.67×10^{-3}	8500	264
	300	6.67×10^{-3}	11625	166
	300	6.67×10^{-2}	20250	132
	300	1.67×10^{-1}	25500	88.4
B	300	6.67×10^{-5}	2480	184
	300	1.67×10^{-4}	2700	220
	300	6.67×10^{-4}	4260	261
	300	1.67×10^{-3}	6220	412
	300	6.67×10^{-3}	11360	442
	300	6.67×10^{-2}	20140	100
	300	1.67×10^{-1}	24700	82

TABLE III (continued)

Process	Temperature °C / Strain Rate S^{-1}		True Strain at 0.1 Plastic Strain (PSI)	Ductility %
C	300	6.67×10^{-5}	1774	322
	300	1.67×10^{-4}	2440	364
	300	6.67×10^{-4}	6660	474
	300	1.67×10^{-3}	8850	440
	300	6.67×10^{-3}	12030	320
	300	6.67×10^{-2}	19250	220
	300	1.67×10^{-1}	21750	114
D	300	6.67×10^{-5}	5220	160
	300	1.67×10^{-4}	6700	230
	300	6.67×10^{-4}	9270	234
	300	1.67×10^{-3}	11250	178
	300	6.67×10^{-3}	17060	110
	300	6.67×10^{-2}	26810	76
	300	1.67×10^{-1}	29680	62

TABLE III (continued)

Process	Temperature °C / Strain Rate S^{-1}		True Strain at 0.1 Plastic Strain (PSI)	Ductility %
E	300	6.67×10^{-5}	3375	158
	300	1.67×10^{-4}	4160	170
	300	6.67×10^{-4}	7180	159
	300	6.67×10^{-3}	16340	124
	300	6.67×10^{-2}	26340	78
	300	1.67×10^{-1}	28800	68
PREVIOUS DATA (ALCAMO) Light Reduction				
	300	6.67×10^{-5}	2000	270
	300	6.67×10^{-4}	4300	330
	300	6.67×10^{-3}	7000	280.6
	300	6.67×10^{-3}	9400	484.4
	300	6.67×10^{-2}	18000	220.6
	300	1.67×10^{-1}	23200	11.04
	300	1.67×10^{-1}	23100	178.8

TABLE III (continued)

Temperature °C / Strain Rate S^{-1}	True Strain at 0.1 Plastic Strain (PSI)	Ductility %
PREVIOUS DATA (GRIDER) Heavy Reduction		
300 6.67×10^{-5}	2800	238
300 6.67×10^{-4}	6300	241
300 6.67×10^{-3}	12700	178
300 1.67×10^{-2}	20600	135
300 1.67×10^{-1}	28300	122

TABLE IV
DATA FOR Al-10%Mg ALLOY IN THE
AS-ROLLED CONDITION

Process	Temperature °C	Strain Rate S^{-1}	True Strain at 0.1 Plastic Strain (PSI)	Ductility %
A	300	6.67×10^{-5}	3615	144
	300	1.67×10^{-4}	3855	178
	300	6.67×10^{-4}	6530	250
	300	1.67×10^{-3}	7820	162
	300	6.67×10^{-3}	11280	144
	300	6.67×10^{-2}	21480	96.8
	300	1.67×10^{-1}	25570	127
B	300	6.67×10^{-5}	2100	238
	300	1.67×10^{-4}	3850	162
	300	6.67×10^{-4}	7100	172
	300	1.67×10^{-3}	9280	172
	300	6.67×10^{-3}	14680	194
	300	6.67×10^{-2}	23480	83
	300	1.67×10^{-1}	25480	88

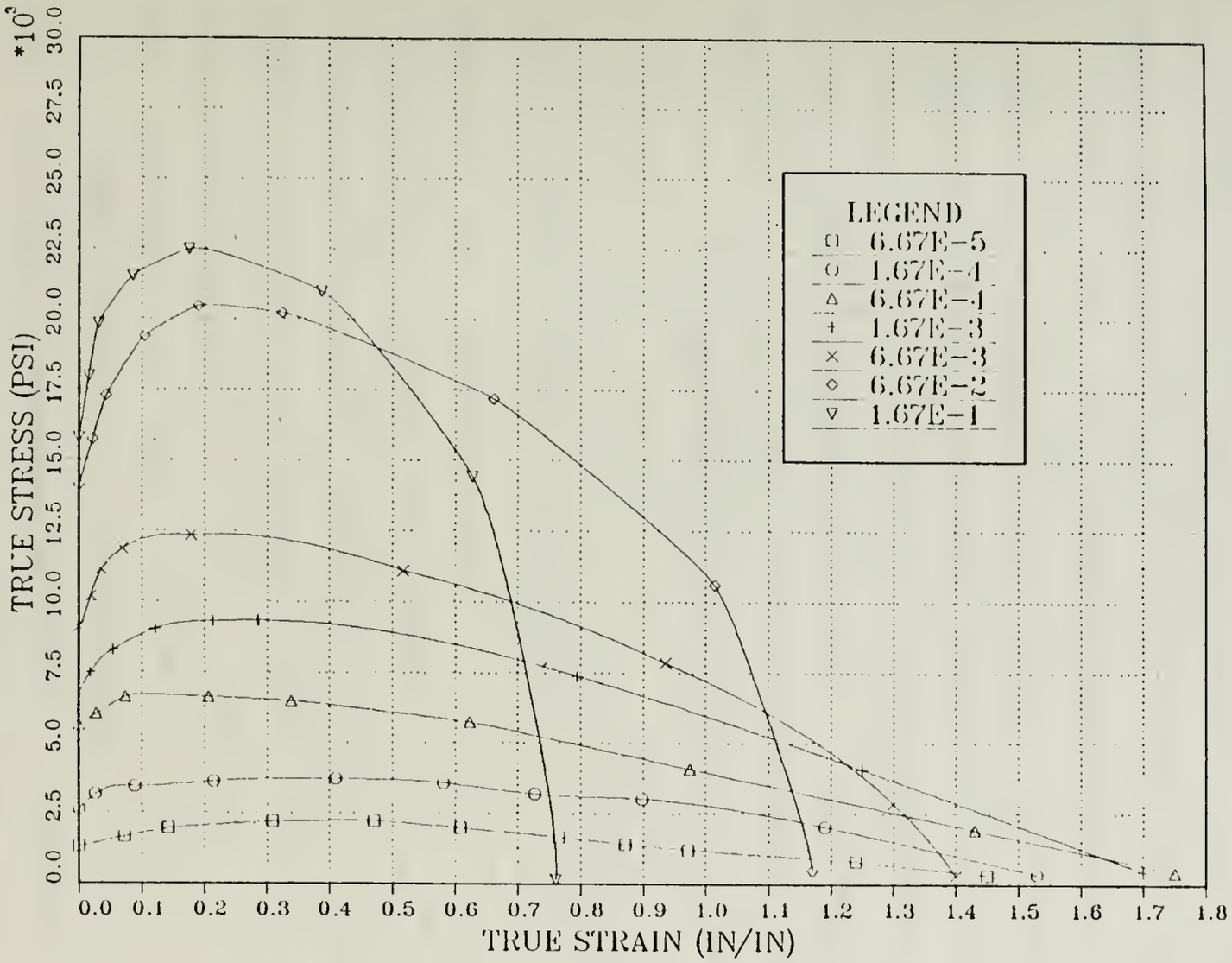

Figure 4.1 True stress vs. true strain for tensile testing conducted at 300°C for an Al-10Mg-0.1Zr alloy. Specimen was solution treated at 440°C for 40 hours, hot worked, resolution treated at 440°C for 1 hour, oil quenched, warm rolled using process C as described in Table II.

Table III shows maximum elongations occurring at strain rates of $6.67 \times 10^{-3}\ S^{-1}$ to $6.67 \times 10^{-4}\ S^{-1}$ this agrees with Grider's, Hartman's and Alcamo's results [Ref. 3, Ref. 15, Ref. 7]. Figure 4.1 clearly shows that at lower strain rates a lower strength is realized and the same was observed for the other processes investigated.

In comparing process A (heavy reduction) with process B (light reduction), shown in Table III, process A is stronger than the same alloy rolled to the same total true strain of 2.5 using process B. This is also evident in the results obtained by Grider [Ref. 3] and Alcamo [Ref. 7] (see Table III) and lends confidence to both data sets.

B. SOLUTION TREATMENT

The initial thermomechanical process conducted was similar to the schematic shown in Figure 3.1; the only difference was that the material was solution treated at 440° C for 5 hours and then at 480°C for 19 hours. The material was upset forged (hot worked) at 480°C for one hour and then vigorously oil quenched. Initial treatment at 440°C was done in an attempt to reduce or avoid hot shortness by dissolving the non-equilibrium eutectic [Ref. 3]. Subsequent treatment at 480°C was expected to accelerate the homogenization of the Mg as indicated by Grider [Ref. 3]. However, during hot working with a platen temperature of 480° C, a billet showed signs of liquation near the top

platen. This resulted in a brittle fracture. Scanning electron microscopy shown in Figure 4.2 revealed intergranular cracking due to partial melting along a grain boundary; this is likely the result of inverse segregation; this phenomenon was also reported by Grider [Ref. 3] and Klankowski [Ref. 18]. McNelley and Lee [Ref. 26] reported that the Beta phase in the as-cast microstructure formed along the grain boundaries due to the non-equilibrium solidification resulting in a nonhomogeneous structure. During the hot working, inhomogeneous Mg distribution due to the non-equilibrium solidification structure likely resulted in hot shortness and cracking of the billet during upset forging. To alleviate this cracking problem, the thermomechanical process was changed (see Figure 3.1). The solution treatment temperature was reduced to 440° C and solutioning time increased to 40 hours. A sufficiently homogenized structure was realized because of the longer solution treatment time and a diminished tendency towards hot shortness was obtained. [Ref. 18] No other brittle fractures occurred.

C. WARM ROLLING

1. Total Strain (1.5 vs 2.5)

Thermomechanical processes A, B and C, as described in Table II, involved warm rolling to nominal true strain of 2.5 and processes D and E represent a nominal true strain of

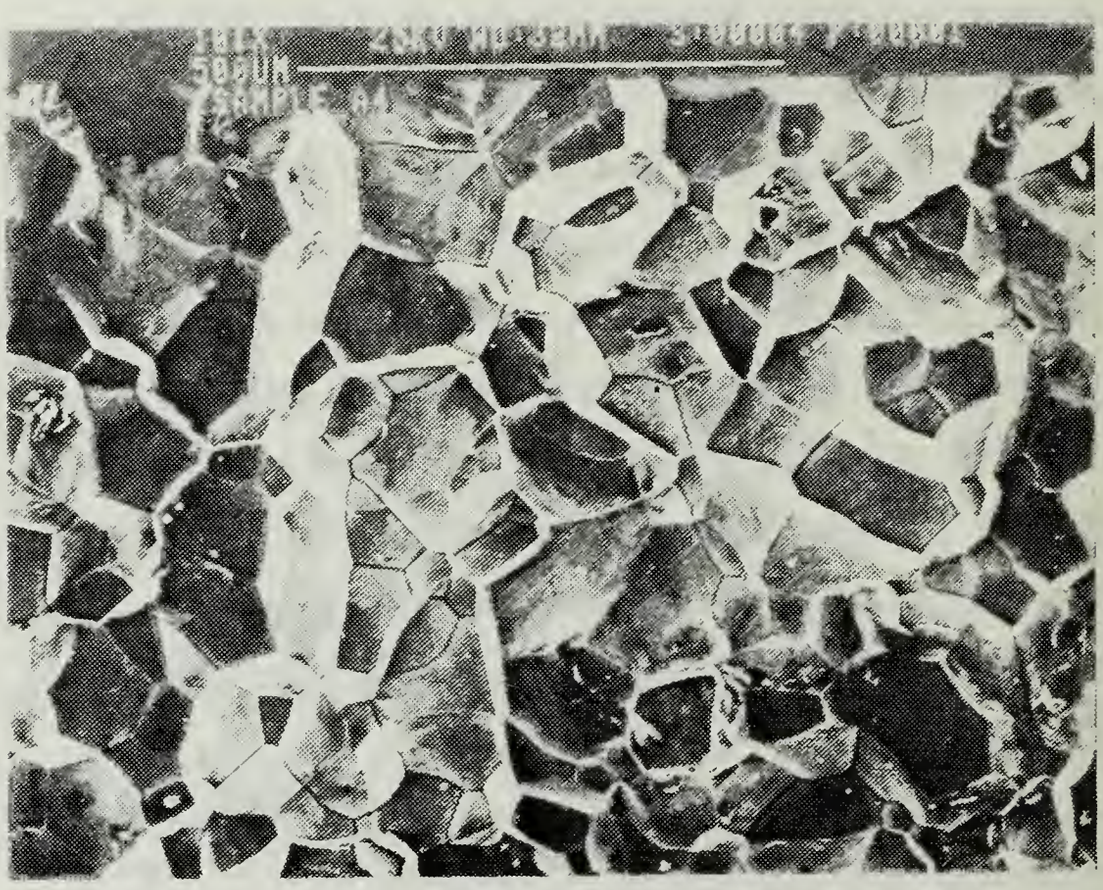

Figure 4.2 SEM micrograph of Al-10Mg alloy during hot working at 480°C. Intergranular cracking occurred due to partial melting along grain boundaries.

1.5. Overall, the more severly worked material (processes B and C) exhibited a much higher warm-temperature ductility than the material strained to 1.5. As shown in Figure 4.3, processes B and C resulted in peak ductilities of 442% and 474%, respectively, and in Figure 4.4 processes D and E showed peak ductilities of 234% and 170%.

Process A yielded a ductility of only 264%. This was unexpected because TEM micrographs in Solomos work [Ref. 27] revealed a very fine subgrain size and Figure 4.5 shows that the m value is greater than 0.4. Based on classical superplastic behavior, these results should have achieved a higher ductility.

The cause of this low ductility was believed at first to be from damaged $ZrAl_3$ particles resulting from the heavy reduction per pass during the warm rolling phase of process A. These cracked $ZrAl_3$ particles would become void initiation sites which could cause premature fracture and hence low ductility. However, subsequent optical and SEM microscopy shown in part F of this chapter did not support this reasoning. Increased reduction per pass and short reheat times likely resulted in a higher dislocation density, possibly less beta precipitate and lessened extent of continuous recrystallization, i.e. insufficient misorientation between adjacent grains for boundary sliding. Table III shows that the material used in process A is stronger and less ductile. Further study is required in this area.

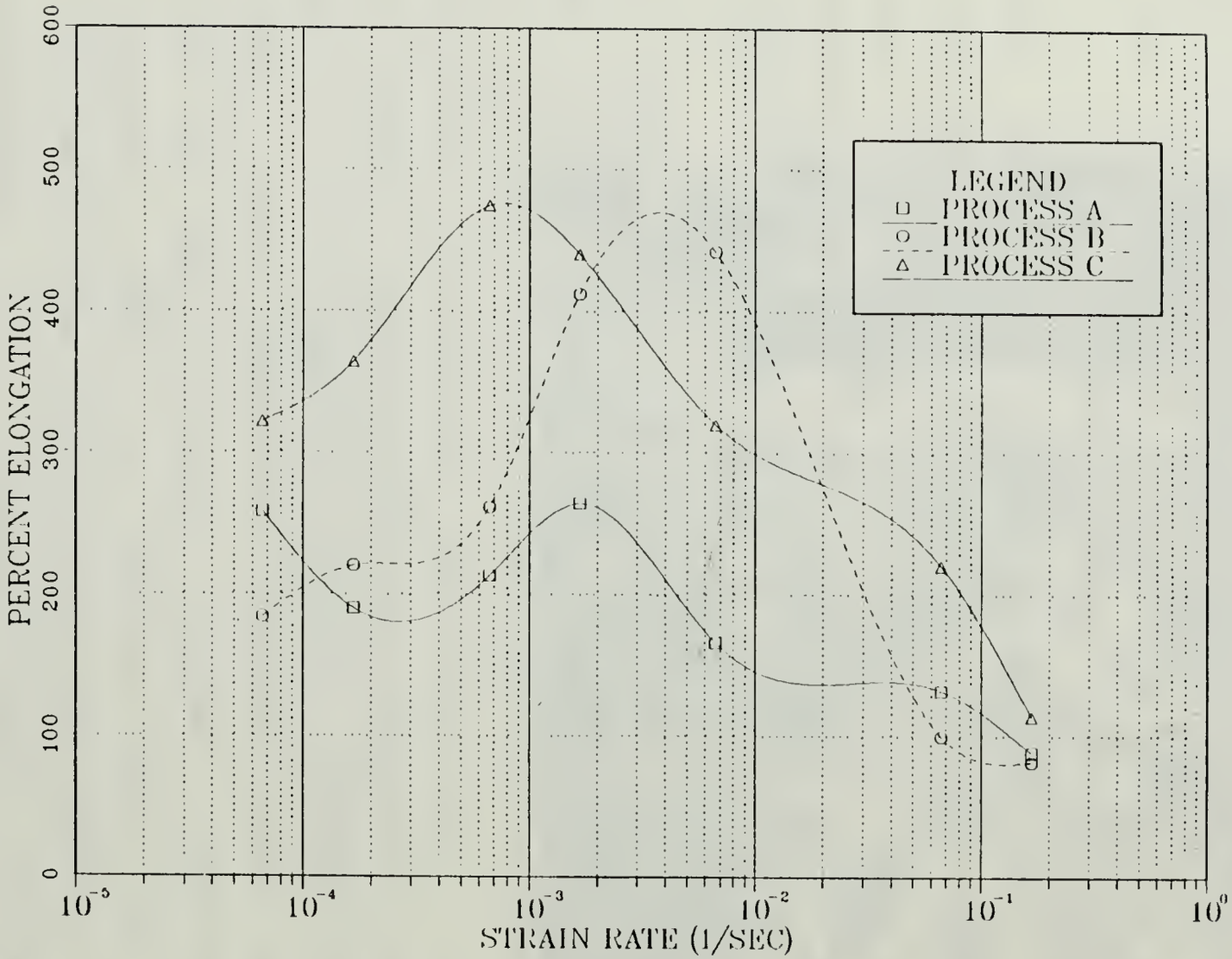

Figure 4.3 Ductility vs. strain rate for Al-10Mg-0.1Zr alloy corresponding to Figure 4.5. Tension treating was done at 300°C with strain rates varying from $6.67 \times 10^{-5} S^{-1}$ to $1.67 \times 10^{-1} S^{-1}$. Specimens were warm rolled at 300°C to a total nominal true strain of 2.5 using processes A, B and C.

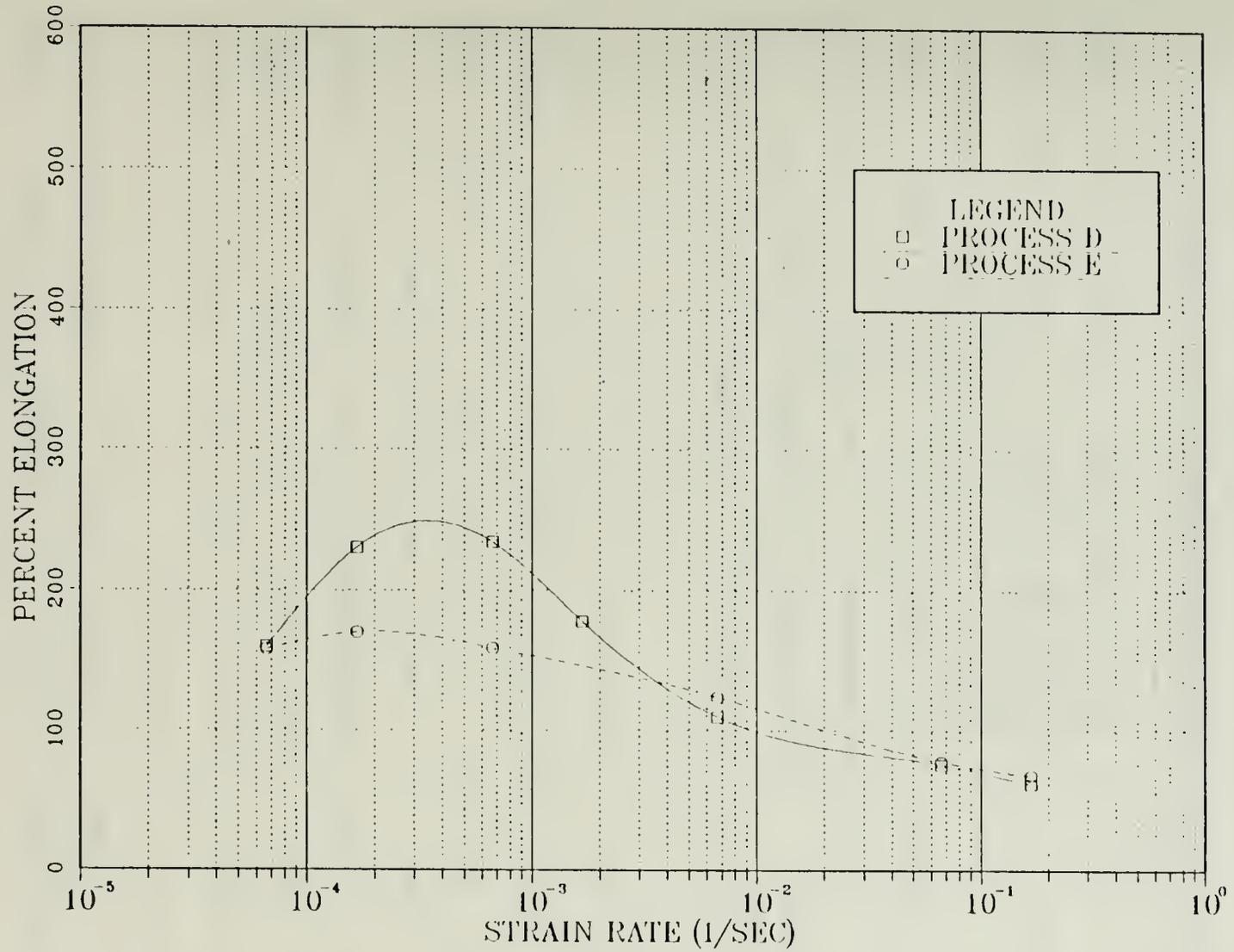

Figure 4.4 Ductility vs strain rate for the Al-10Mg-0.1Zr alloy corresponding to Figure 4.6. Tension tested at 300°C with strain rates varying from $6.67 \times 10^{-5} S^{-1}$ to $1.67 \times 10^{-1} S^{-1}$. Specimens were warm rolled at 300°C to a total nominal true strain of 1.5 using processes D and E.

In Figures 4.5 and 4.6, data for true stress at 0.1 strain versus strain rate clearly shows that the material weakens as the total strain is increased from 1.5 to 2.5.

2. Strain Rate (Light Reduction Verses Heavy Reduction)

Processes A and B were warm rolled to a total nominal strain of 2.5 with process A being the heavy reduction schedule and process B the light reduction schedule. Figure 4.5 shows that at lower strain rates (6.67×10^{-5} S^{-1}) process A appears to be strain hardening to a greater extent. This suggests increased coarsening. At higher strain rates (1.67×10^{-1} S^{-1}), processes A and B strain harden at the same rate.

The heavily reduced material (process A) is strain hardening faster than process B because more stored energy is present, causing the grains to grow out faster and coarsen. This could be one reason why process A has low ductility. Further investigation of true stress vs strain rate curves at .02 and .2 strain (see Figure 4.7) clearly show that again process A at lower strain rates is strain hardening faster than process B.

In the case of process D and E the same results were observed except that overall flow stress values were higher than for processes A and B.

3. Reheating Time (4 min. versus 30 min.)

Process B was warm rolled with a 4 minute reheat time per pass and process C was warm rolled with a 30 minute

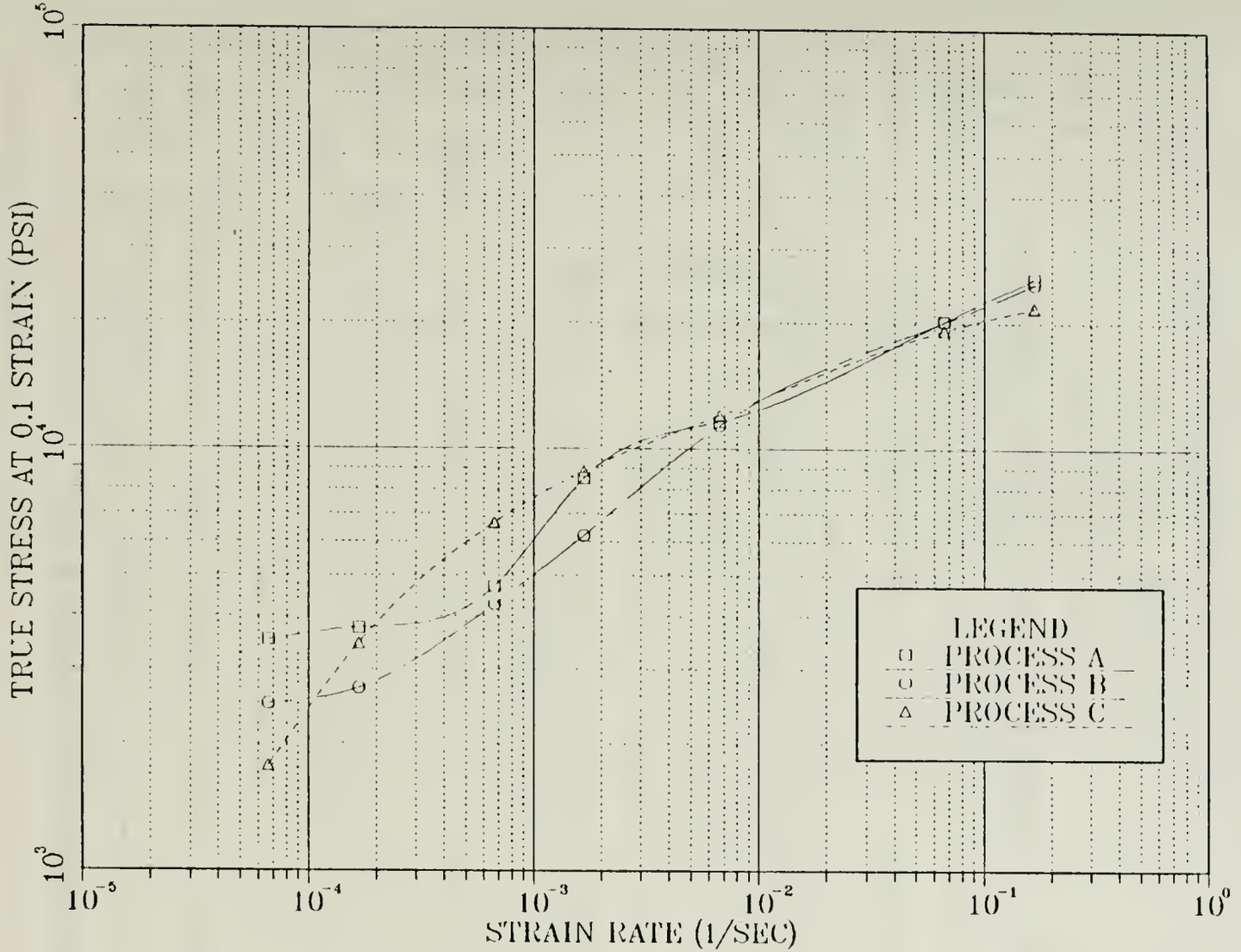

Figure 4.5 True stress at 0.1 strain vs. strain rate for Al-10Mg-0.1Zr alloy tension tested at 300°C with strain rates varying from $6.67 \times 10^{-5} S^{-1}$ to $1.67 \times 10^{-1} S^{-1}$. Specimens were warm rolled at 300°C to a total nominal true strain of 2.5 using processes A, B and C.

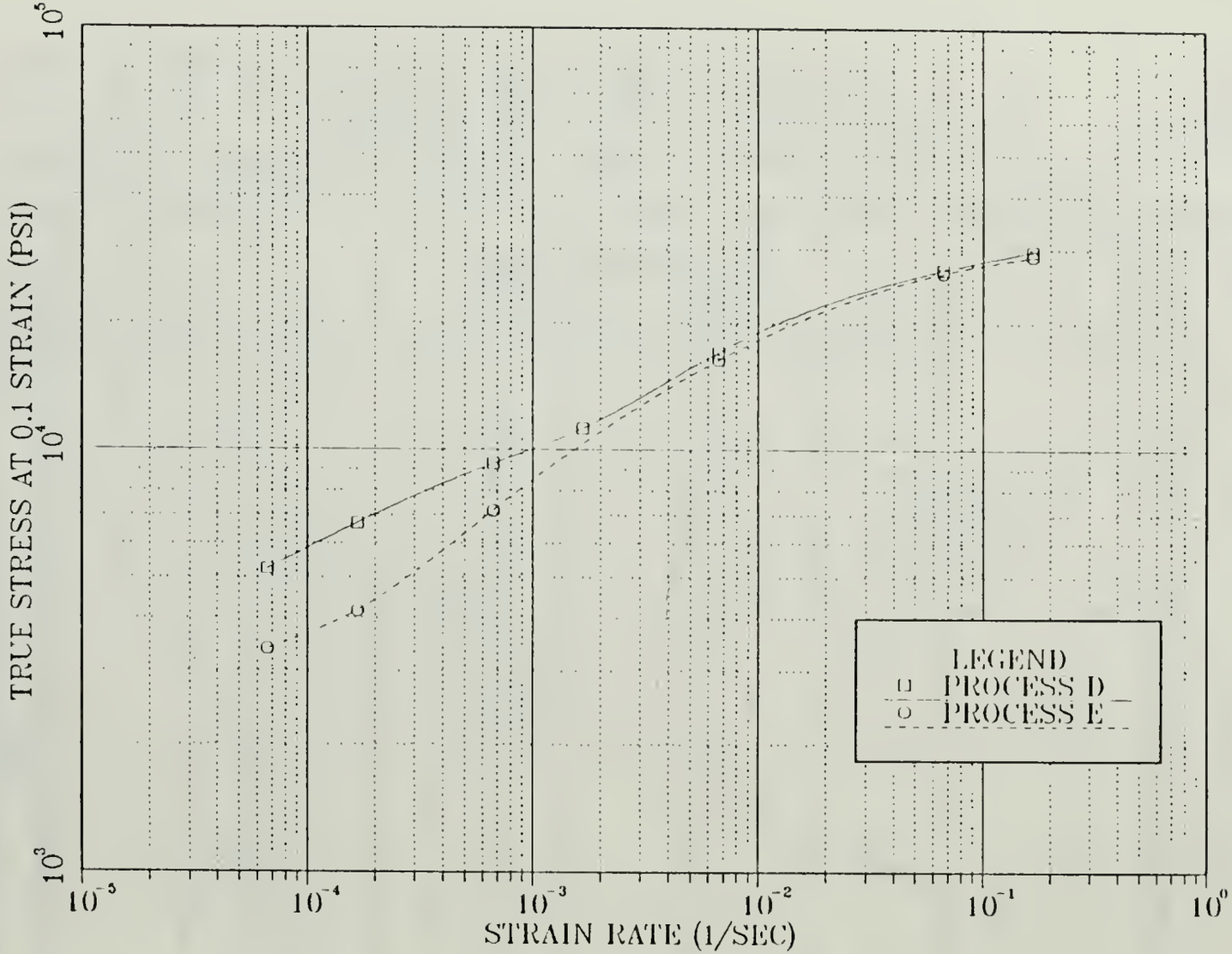

Figure 4.6 True stress at 0.1 strain vs. strain rate for Al-10Mg-0.1Zr alloy tension tested at 300°C with strain rates varying from $6.67 \times 10^{-5} S^{-1}$ to $1.67 \times 10^{-1} S^{-1}$. Specimens were warm rolled at 300°C to a total nominal true strain of 1.5 using processes D and E.

reheat time per pass. Figure 4.5 clearly shows higher m values at the lower strain rates, $6.67 \times 10^{-5}\ S^{-1}$ to $6.67 \times 10^{-4}\ S^{-1}$, for process C and for process B the highest m value occurred at strain rates $6.67 \times 10^{-4}\ S^{-1}$ to $6.67 \times 10^{-2}\ S^{-1}$. Each of these peak m values coincide with peak ductilities shown in Figure 4.3.

Comparing Figure 4.7 with Figure 4.8 reveals that process B is strain hardening at strain rate $6.67 \times 10^{-5}\ S^{-1}$ whereas, process C shows less. But as the strain rate is increased, process C begins to strain harden at a rate faster and is very similar at higher strain rates to process B. This likely is because of the longer reheating schedule.

At lower strain rates for process C, the grains begin to coarsen, the m value increases, and the overall flow stress of the material becomes higher. For process B, a finer grain structure evolves with a lower true stress value and a higher m value for strain rates varying from $6.67 \times 10^{-4}\ S^{-1}$ to $1.67 \times 10^{-3}\ S^{-1}$ as compared to process C. Figure 4.3 supports these results in that the peak ductilities occur at lower strain rates for process C and at higher strain rates for process B.

It is thought that the slow warm rolling schedule of process C does not yield as fine a grain structure initially, but a more stable structure because of a more fully recrystallized structure developed during the warm rolling.

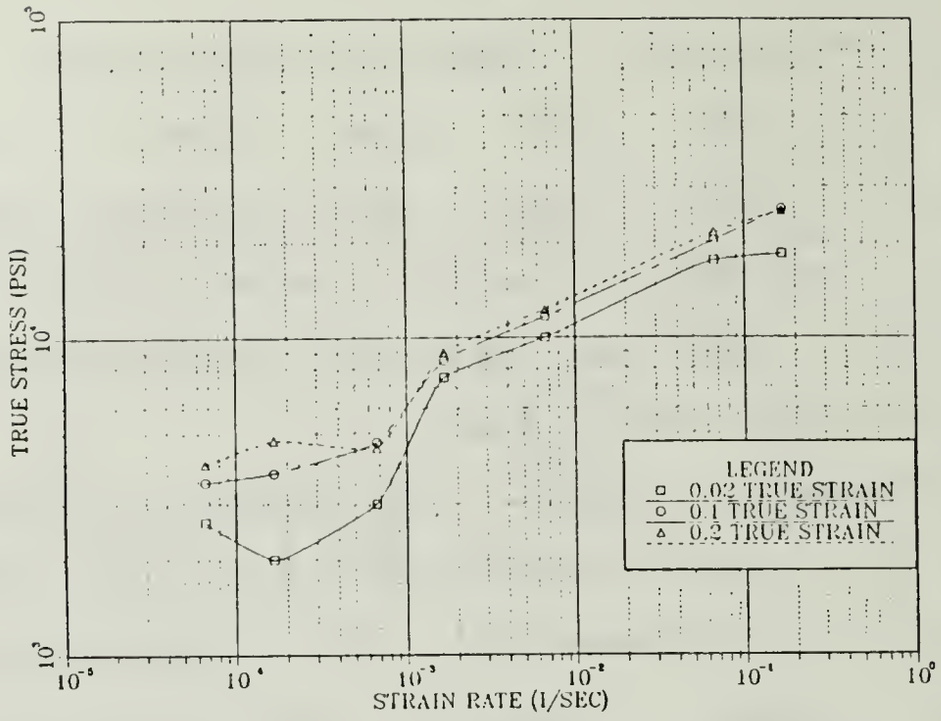

a

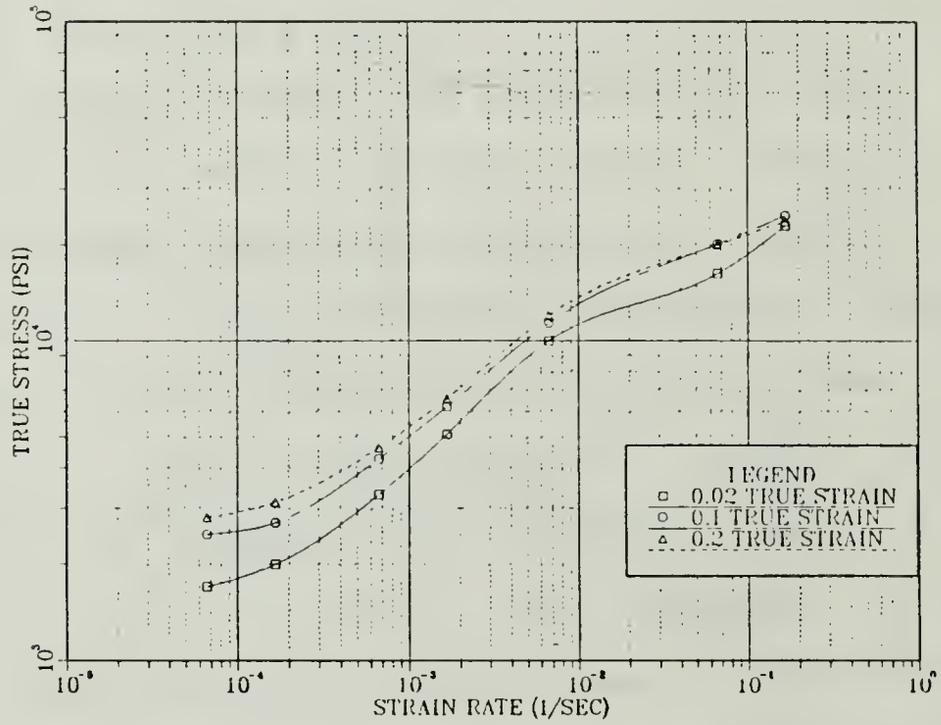

b

Figure 4.7 True stress at 0.02, 0.1, and 0.2 strain vs. strain rate for Al-10Mg-0.1Zr alloy, tension tested at 300°C with strain rates varying from $6.67 \times 10^{-5} S^{-1}$ to $1.67 \times 10^{-1} S^{-1}$. Material was warm rolled to a total nominal strain of 2.5 using: a) process A, and b) process B.

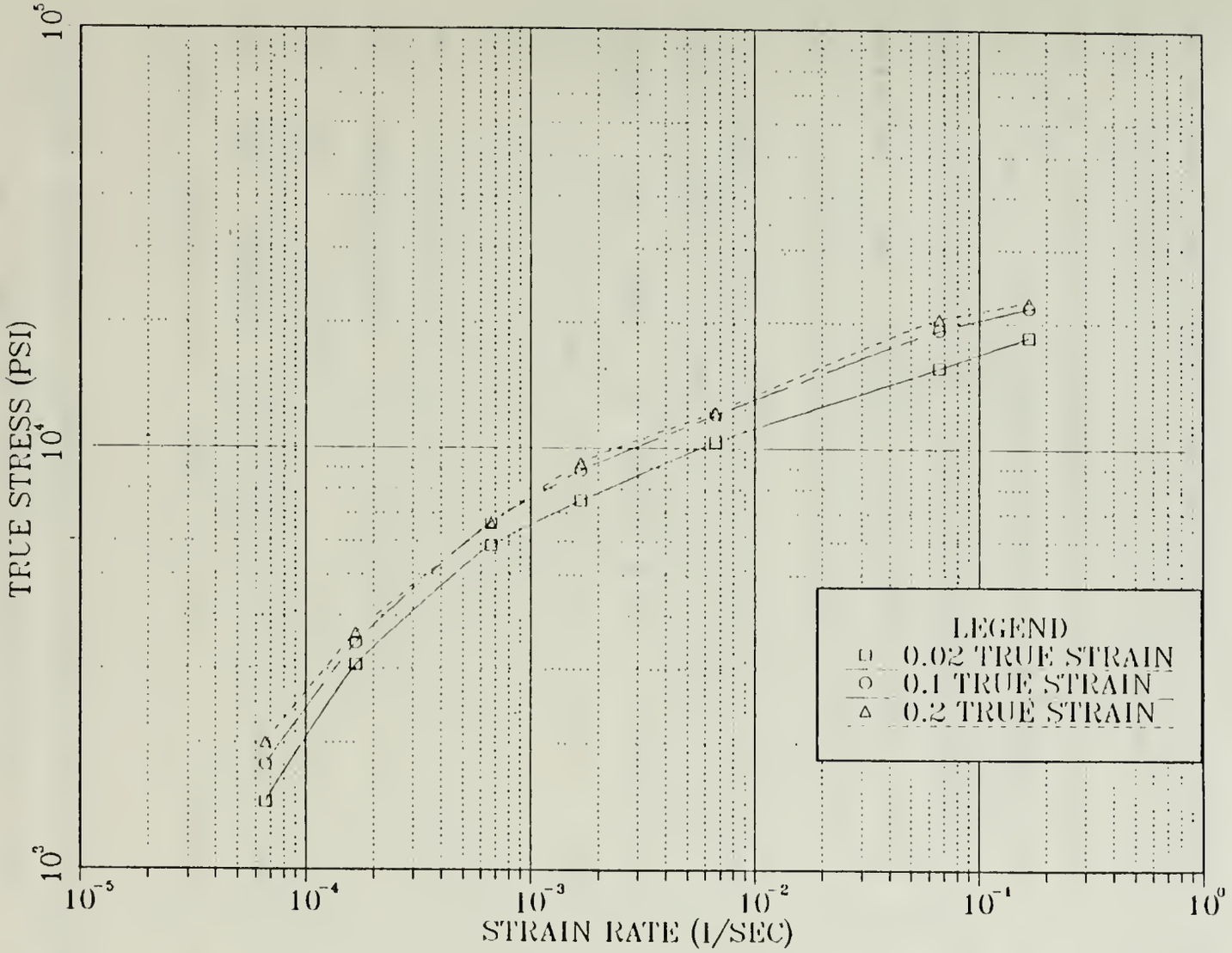

Figure 4.8 True stress at 0.02, 0.1 and 0.2 true strain vs. strain rate for the Al-10Mg-0.1Zr alloy tension tested at 300°C with strain rates varying from $6.67 \times 10^{-5} S^{-1}$ to $1.67 \times 10^{-1} S^{-1}$. Material was warm rolled at 300°C to a total nominal strain of 2.5 using process C.

D. ALLOYING VARIABLES

The addition of magnesium (8 to 10 wt.%) to aluminum alloys increases the strength of the alloy, decreases its weight and enhances its superplastic properties as shown here. Too much magnesium may result in sufficient beta phase, which approaches the stoichiometric ratio Al_8Mg_5, to render the alloy brittle at ambient temperature [Ref. 15]. In the ternary alloy, the addition of zirconium facilitates achieving a fine grain size and allows for increased microstructural stability during superplastic forming [Ref. 15]. The ternary alloy, (Al-10%Mg-0.1Zr) exhibited substantially higher ductilities (442%) at strain rates varying from $6.67 \times 10^{-4}\ S^{-1}$ to $6.67 \times 10^{-3}\ S^{-1}$ than the binary alloy (Al-10%Mg) (194%) for process B (see Tables III and IV).

An interesting result was obtained from process A of both alloys, in that the ductilities were approximately the same for strain rates $6.67 \times 10^{-3}\ S^{-1}$ to $1.67 \times 10^{-1}\ S^{-1}$ and the peak ductilities were nearly identical except that the ternary alloy peaked at a slower strain rate than the binary alloy.

Higher ductilities obtained in process B of the ternary alloy were expected but not obtained in the binary alloy. The m values in Figures 4.5 and 4.9 for process A were similar and coincided with occurrence of peak ductilities in

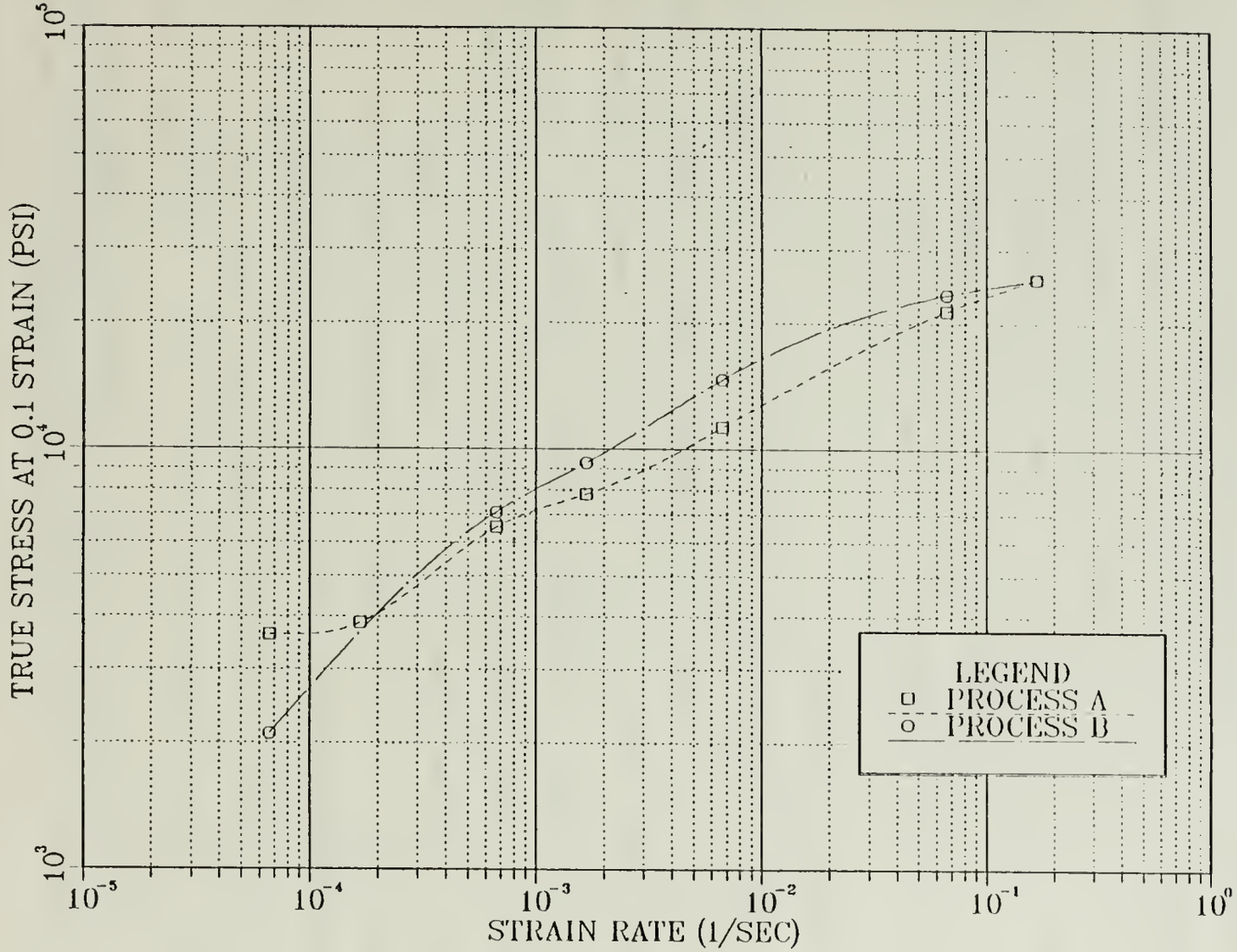

Figure 4.9 True stress at 0.1 strain vs. strain rate for the binary Al-10Mg alloy tension tested at 300°C. Specimens were warm rolled at 300°C using processes A and B.

Figures 4.3 and 4.10. The reason for the uncharacteristically low ductility values obtained from the ternary alloy in process A again is unknown and further investigation is required of this phenomenon.

Comparing Figures 4.5 and 4.9 shows that binary material is stronger than the ternary alloy at warm temperature and Figures 4.3 and 4.10 reveal higher ductility for the ternary alloy which was expected based on the assumption that the ternary addition stabilized a finer grain size.

E. OPTICAL MICROSCOPY

Optical micrographs were obtained of warm rolled materials experiencing the different warm rolling processes, all specimens revealed an elongated, somewhat banded grain structure with a second phase uniformly distributed throughout the structure. Figure 4.11 shows the effect of process A on the material. This specimen reveals a very fine Beta phase that is not as uniformly distributed as in the other processes. Process B is illustrated in Figure 4.12, and shows a coarser second phase that is also more uniformly distributed than in process A. In Figure 4.13 a banded structure is still seen, however the Beta phase is larger than what is seen in Figures 4.11 and 4.12 because of grain coarsening. This was expected because in process C, the material was reheated 30 minutes between each rolling

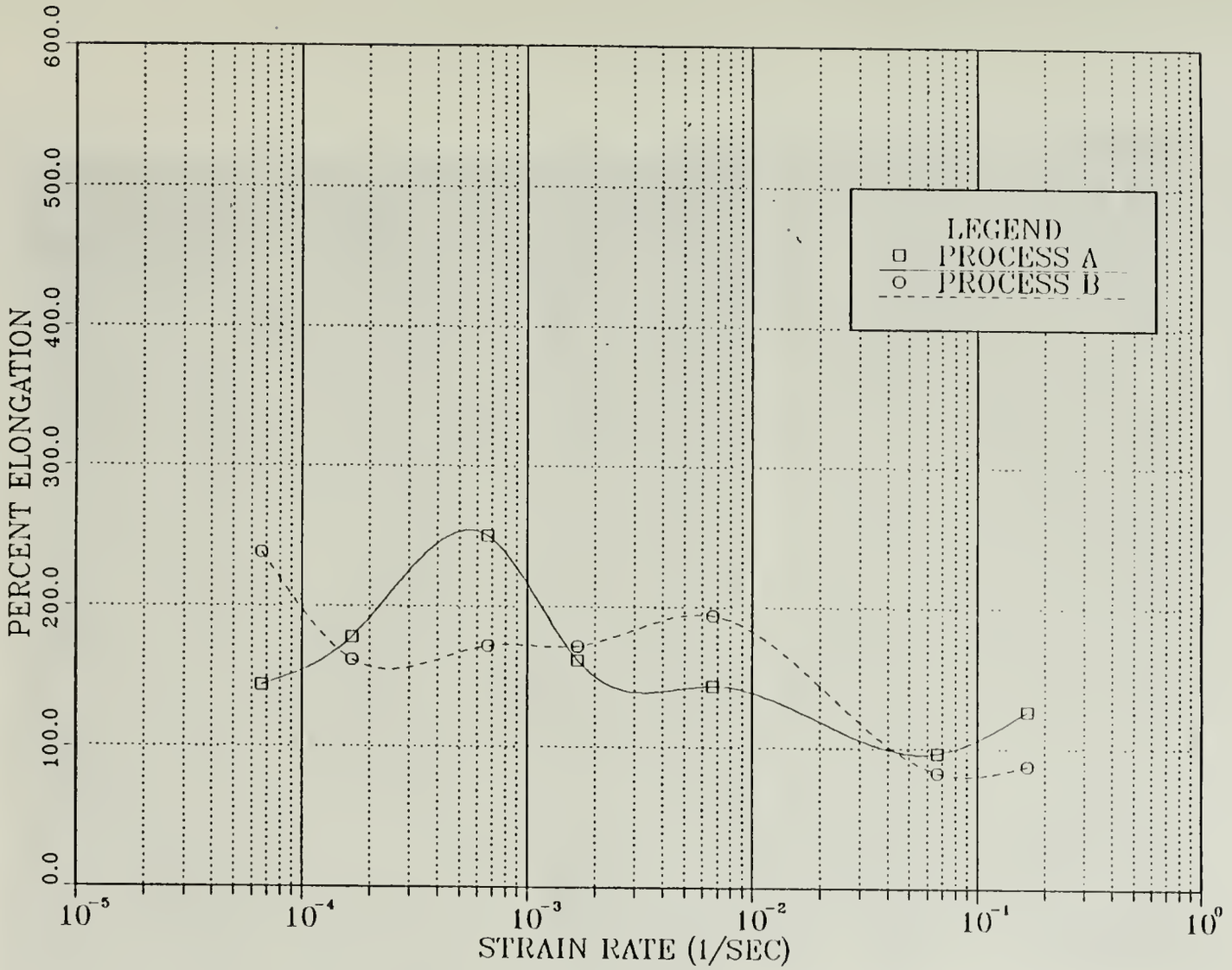

Figure 4.10 Ductility vs. strain rate for the binary Al-10Mg alloy tension tested at 300°C with strain rates varying from $6.67 \times 10^{-5} S^{-1}$ to $1.67 \times 10^{-1} S^{-1}$. Specimens were warm rolled to a total nominal strain of 2.5 using processes A and B as described in Table II.

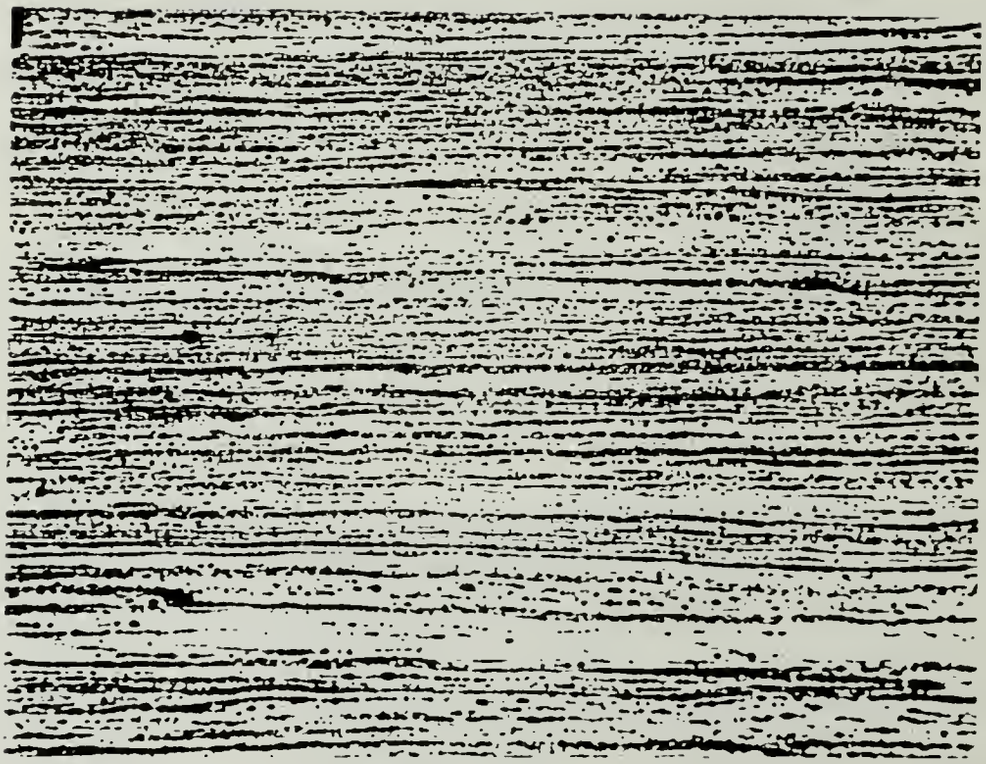

Figure 4.11 Optical Micrograph of Al-10Mg-0.1Zr alloy after warm rolling using process A (500x) in the longitudinal direction.

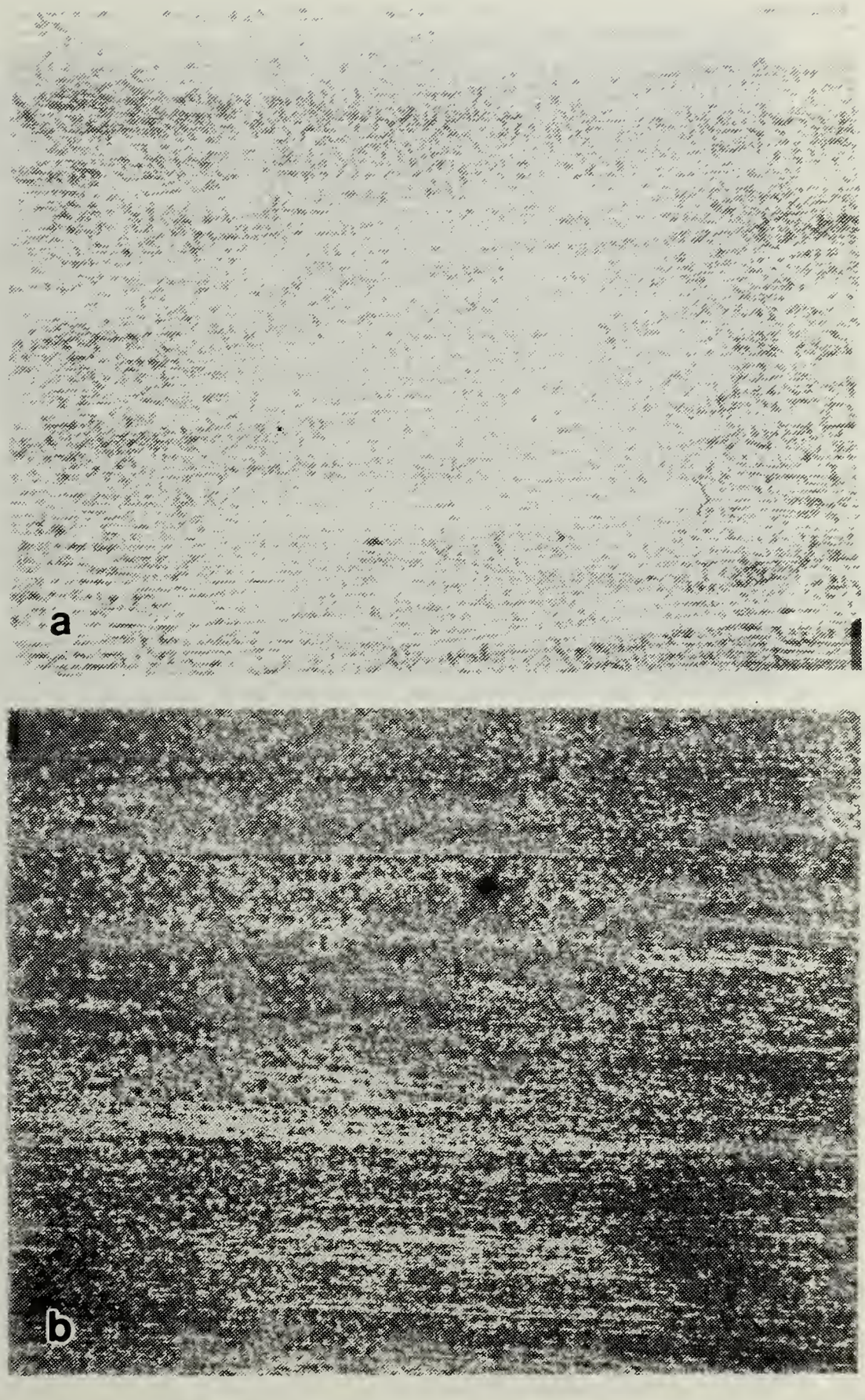

Figure 4.12 Optical micrograph of Al-10Mg-0.1Zr alloy after warm rolling using process B (500x)
(a) Transverse direction
(b) Longitudinal direction

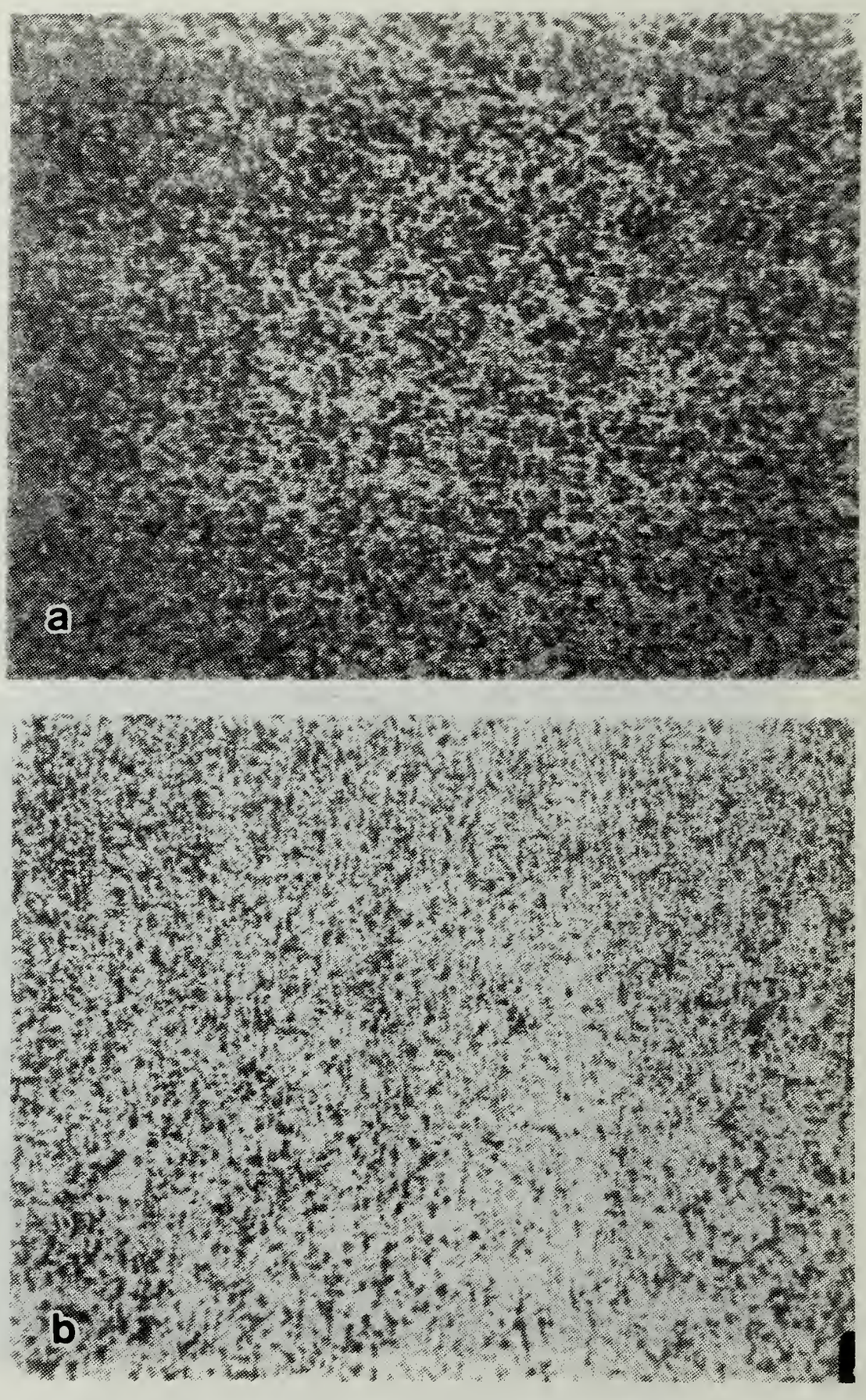

Figure 4.13 Optical micrograph of Al-10Mg-0.1Zr alloy after warm rolling using process C (500x)
(a) Transverse direction
(b) Longitudinal direction

pass, allowing the C time to grow and coarsen. Grider [Ref. 3] reported similar observations for the heavy and light reduction rolling schedules.

F. SCANNING ELECTRON MICROSCOPY

SEM micrographs of samples processed by methods A and B and then deformed at 300°C, are shown in Figure 4.14. This figure reveals a fine grain structure due to grains emerging by grain boundary sliding. Process B achieved an elongation of 442% and process A achieved an elongation of only 264% even though the grain size in process A is similar to process B. It was thought that damaged $ZrAl_3$ particles may have caused premature fracture in process A material. However, analysis done by Solomos [Ref. 27] indicated that no $ZrAl_3$ particles were associated with voids. The underlying reason for this behavior is not known. These microscopy results suggest a refined structure has evolved; however, if continuous recrystallization is occurring, the short reheating may not have allowed sufficient time for a structure capable of sustaining grain boundary sliding to develop. A micrograph of process C, shown in Figure 4.15, shows that grain coarsening is beginning to appear. These grains are larger because of the longer reheat times used in process C. An elongation of 474% was attained with this specimen.

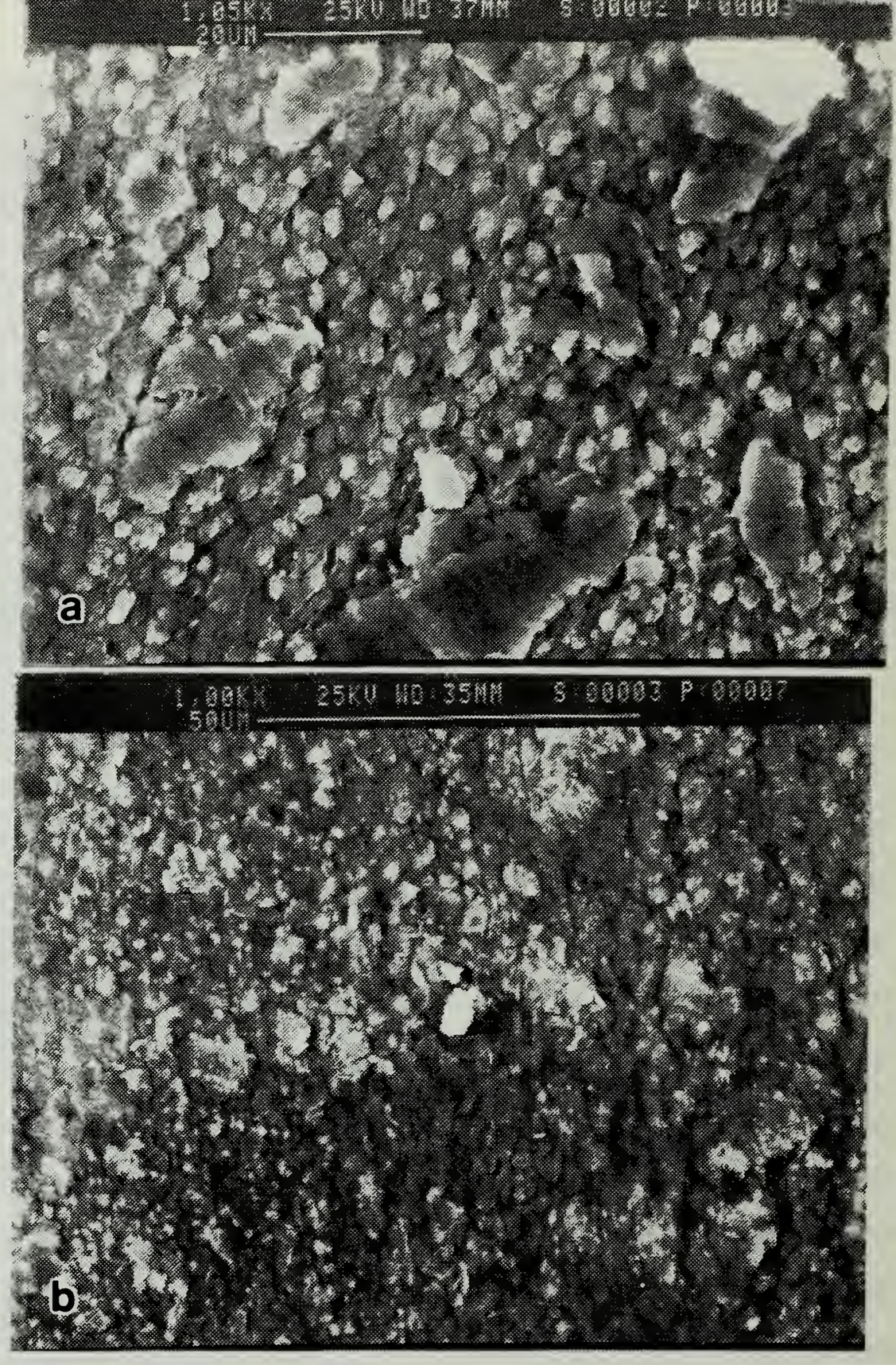

Figure 4.14 SEM micrographs of as rolled Al-10Mg-0.1Zr alloy taken near fracture point.

(a) process A tensile tested at 300°C and $1.67 \times 10^{-3} s^{-1}$ strain rate (1000x).

(b) process B tensile tested at 300°C and $6.67 \times 10^{-3} s^{-1}$ strain rate (1000x).

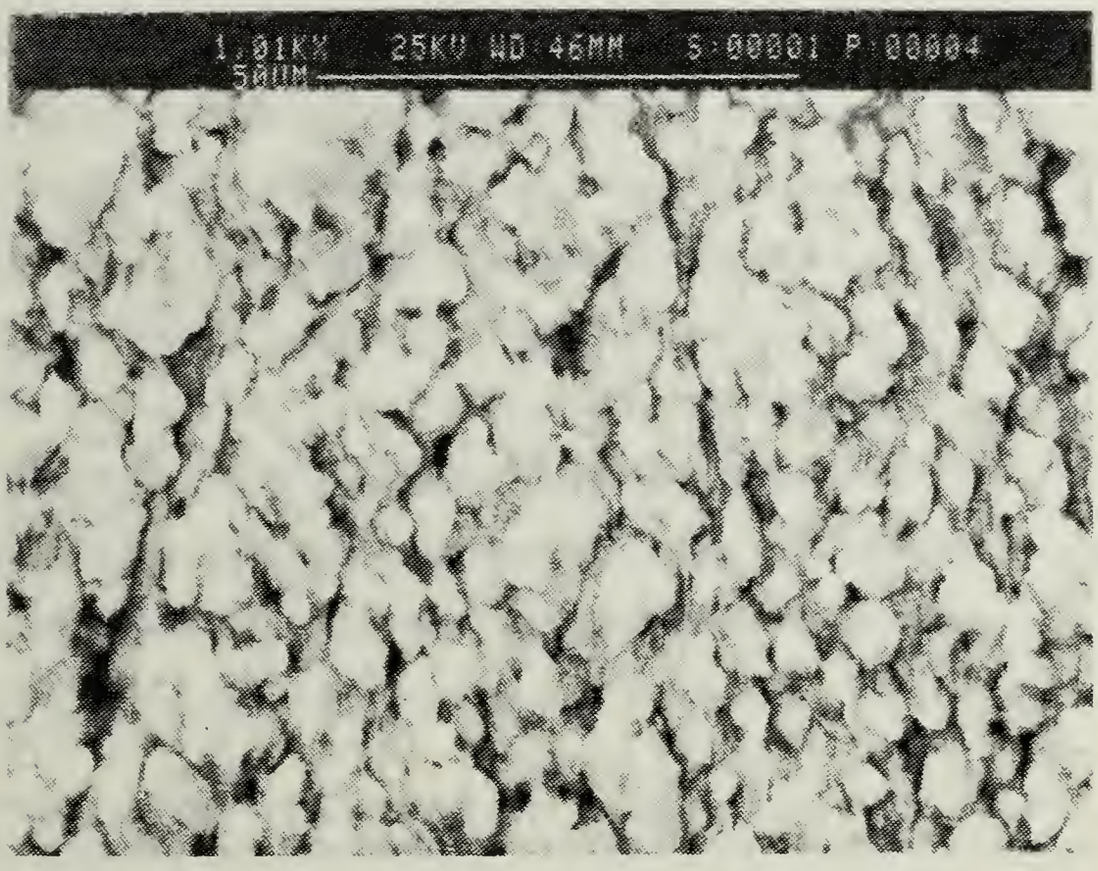

Figure 4.15 SEM micrograph of tension tested Al-10Mg-0.1Zr alloy taken near fracture point of process C. Specimen was tensile tested at 300°C and $6.67 \times 10^{-4} s^{-1}$ strain rate.

V. CONCLUSIONS AND RECOMMENDATIONS

A. CONCLUSIONS

The following conclusions are drawn from this research.

1. Solution treatment of billets conducted at 480°C can cause brittle fracture to occur due to partial melting along the grain boundary in conjunction with inverse segregation.
2. Material warm-rolled to a total true strain of 2.5 using the light reduction schedule, (processes B and C) exhibited much higher ductilities than material warm-rolled to a lesser true strain of 1.5 under the same conditions.
3. The heavy reduction rolling used in process A was less ductile than that achieved using the light reduction rolling of processes B and C.
4. The Al-10Mg-0.1Zr alloy weakens when the total true strain is increased from 1.5 to 2.5.
5. Heavily reduced material (processes A and D) strain hardens faster than lightly reduced material (processes B and E), because more stored energy is present causing the grains to grow out and coarsen.
6. Longer reheating times as compared to shorter reheating times revealed coarser grains, peak ductilites occurring at slower strain rates, and similar m

values. The 30 minute reheat time of process C, achieved the highest percent elongation (474%) for the Al-10Mg-0.1Zr alloy.

7. Approximately the same peak ductilities were obtained for the Binary and Ternary alloys using the heavy reduction schedule process A.
8. Substantially higher percent elongations (442% vs 241%) were achieved using process B (light reduction) in the ternary alloy as compared to the binary alloy.
9. The heavier reduction rolling done in process A resulted in a less uniformly distributed intermetallic beta phase as observed by optical microscopy.

B. RECOMMENDATIONS

The following are recommendations for further study.

1. Conduct the same series of experiments done in this research with an alloy that contains higher amounts of zirconium (>0.1%Zr). This will verify if the additional zirconium is a variable in the mechanical properties of the Al-10Mg alloy.
2. Investigate what effect temperature has on the Al-10Mg-0.1Zr alloy by conducting the same series of tests at a higher temperature and a lower temperature. This will determine if temperature is a variable in the mechanical properties of the alloy.

3. Conduct processes C, D, and E on the Al-10Mg alloy to complete the test matrix.
4. Warm roll the Al-10Mg-0.1Zr alloy using a heavy reduction schedule and a 30 minute reheat time per pass, to study the effect it has on the ductility and strength of this alloy.
5. Use the Differential Scanning Calorimeter (DSC) to simulate time at 300°C without straining the material and compare this to material that was actually strained. This will verify what effect time at temperature has versus strain rate on the ductility of the material.

APPENDIX A

MECHANICAL TEST DATA ON Al-10%Mg-0.1Zr ALLOY

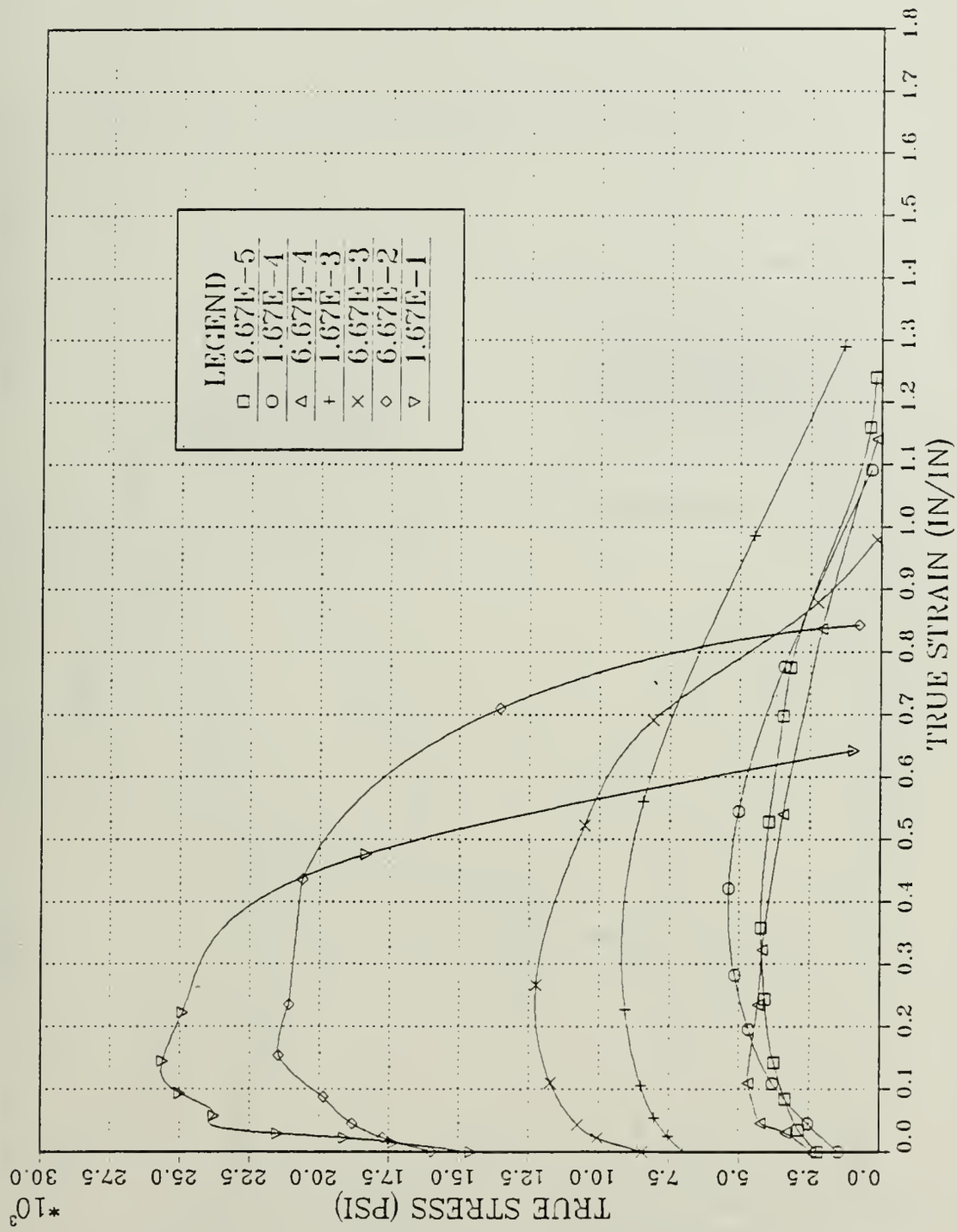

Figure A.1 True stress vs. true strain for tensile testing conducted at 300°C for an Al-10Mg-0.1Zr alloy. Specimen was solution treated at 440°C for 40 hours, hot worked, resolution treated at 440°C for 1 hour, oil quenched, warmed rolled using process A as described in Table II.

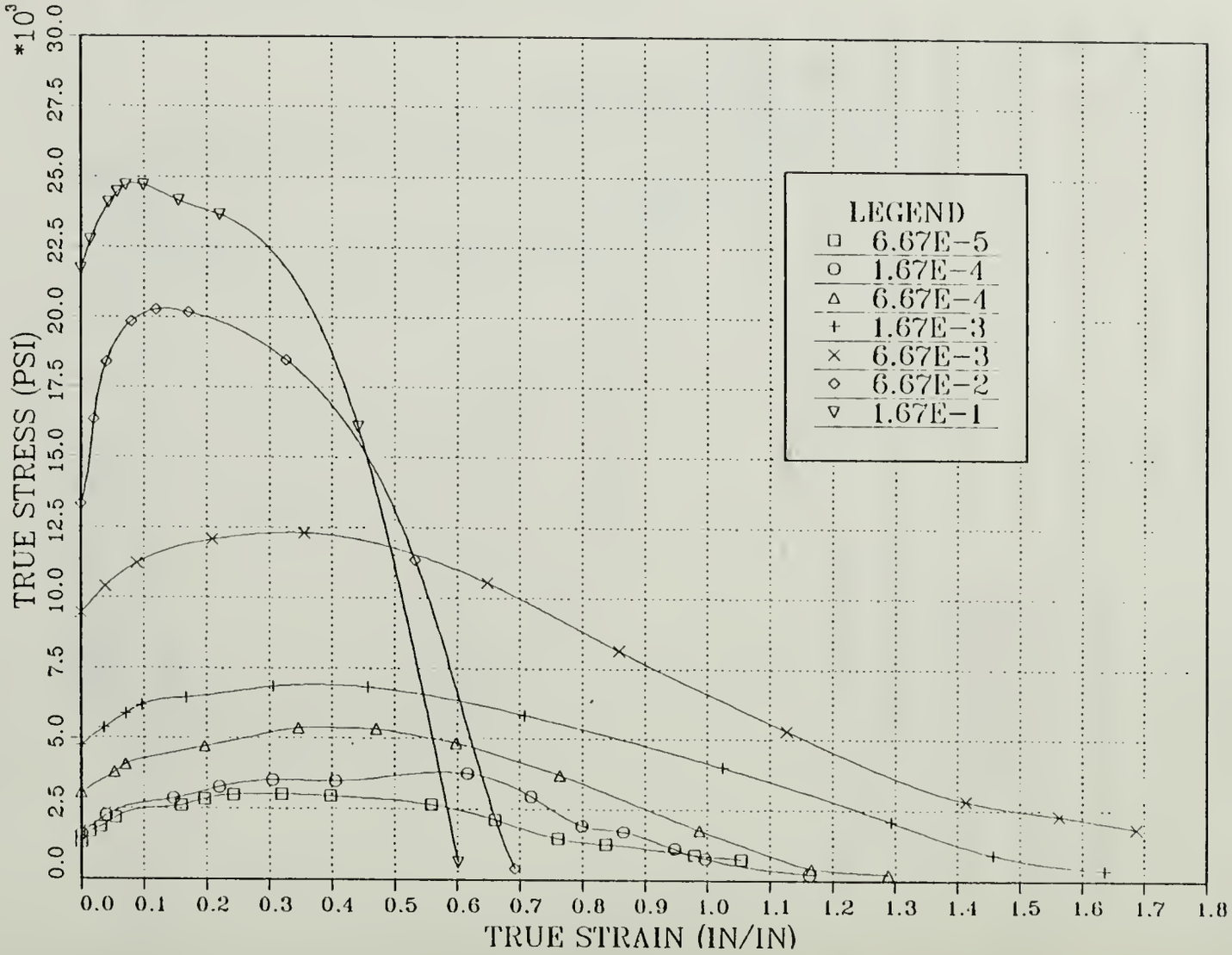

Figure A.2 True stress vs. true strain for tensile testing conducted at 300°C for an Al-10Mg-0.1Zr alloy. Specimen was solution treated at 440°C for 40 hours, hot worked, resolution treated at 440°C for 1 hour, oil quenched, warm rolled using process B as described in Table II.

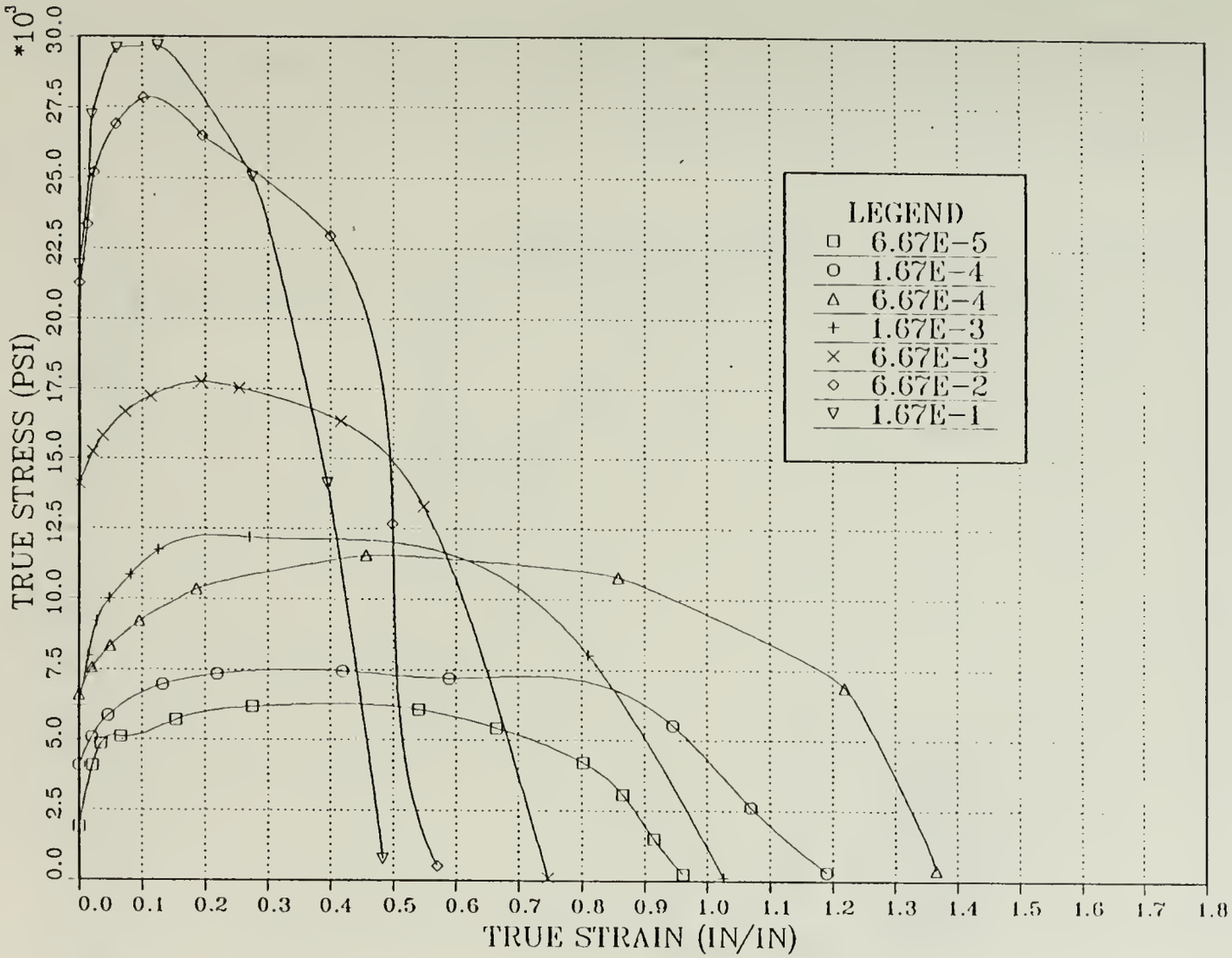

Figure A.3 True stress vs. true strain for tensile testing conducted at 300°C for an Al-10Mg-0.1Zr alloy. Specimen was solution treated at 440°C for 40 hours, hot worked, resolution treated at 440°C for 1 hour, oil quenched, then warm rolled using process D as described in Table II.

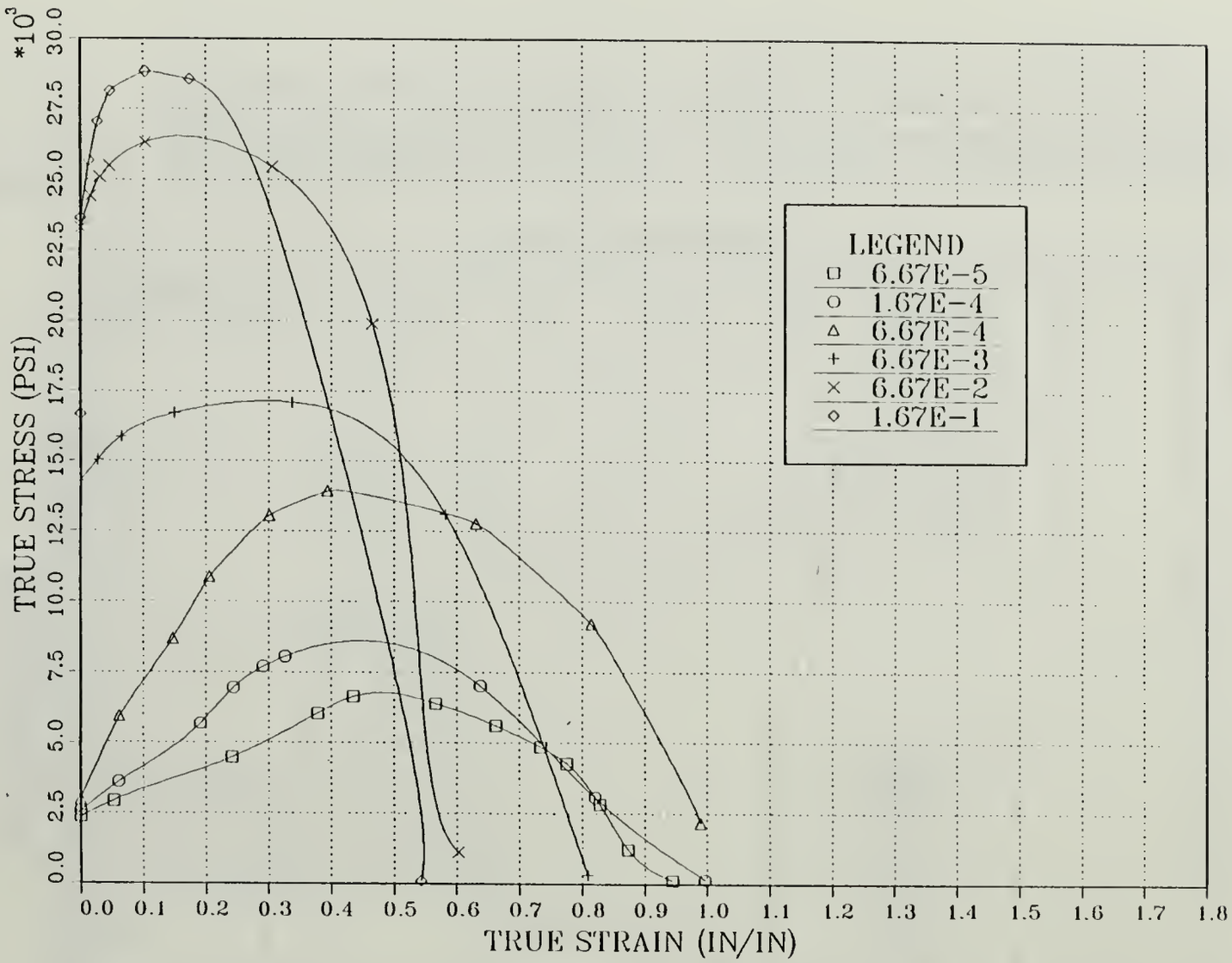

Figure A.4 True stress vs. true strain for tensile testing conducted at 300°C for an Al-10Mg-0.1Zr alloy. Specimen was solution treated at 440°C for 40 hours, hot worked, resolution treated at 440°C for 1 hour, oil quenched, then warm rolled using process E as described in Table II.

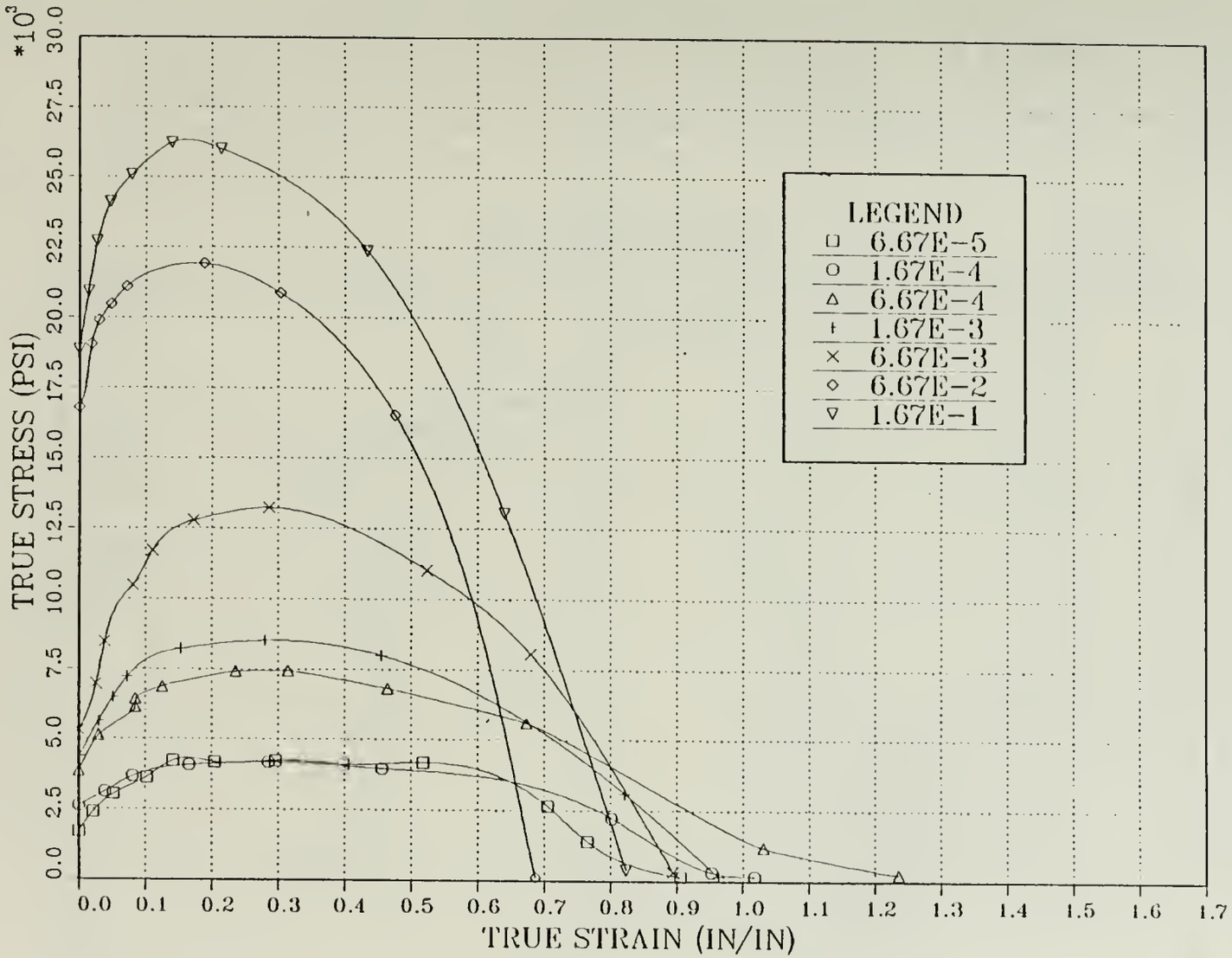

Figure A.5 True stress vs. true strain for tensile testing conducted at 300°C for an Al-10Mg alloy. Specimen was solution treated at 440°C for 40 hours, hot worked, resolution treated at 440°C for 1 hour, oil quenched, then warm rolled using process A as described in Table II.

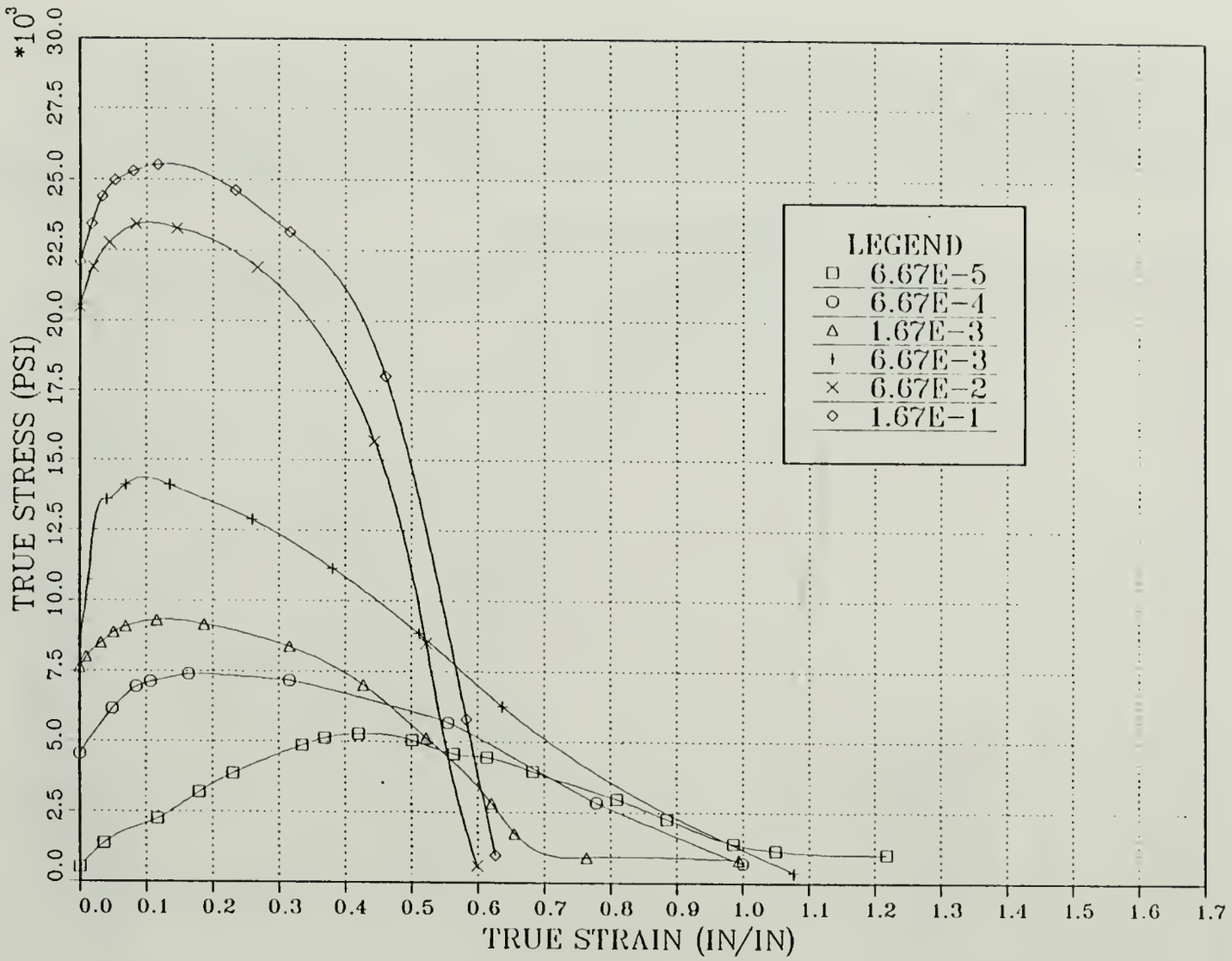

Figure A.6 True stress vs. true strain for tensile testing conducted at 300°C for an Al-10Mg alloy. Specimen was solution treated at 440°C for 40 hours, hot worked, resolution treated at 440°C for 1 hour, oil quenched, then warm rolled using process B as described in Table II.

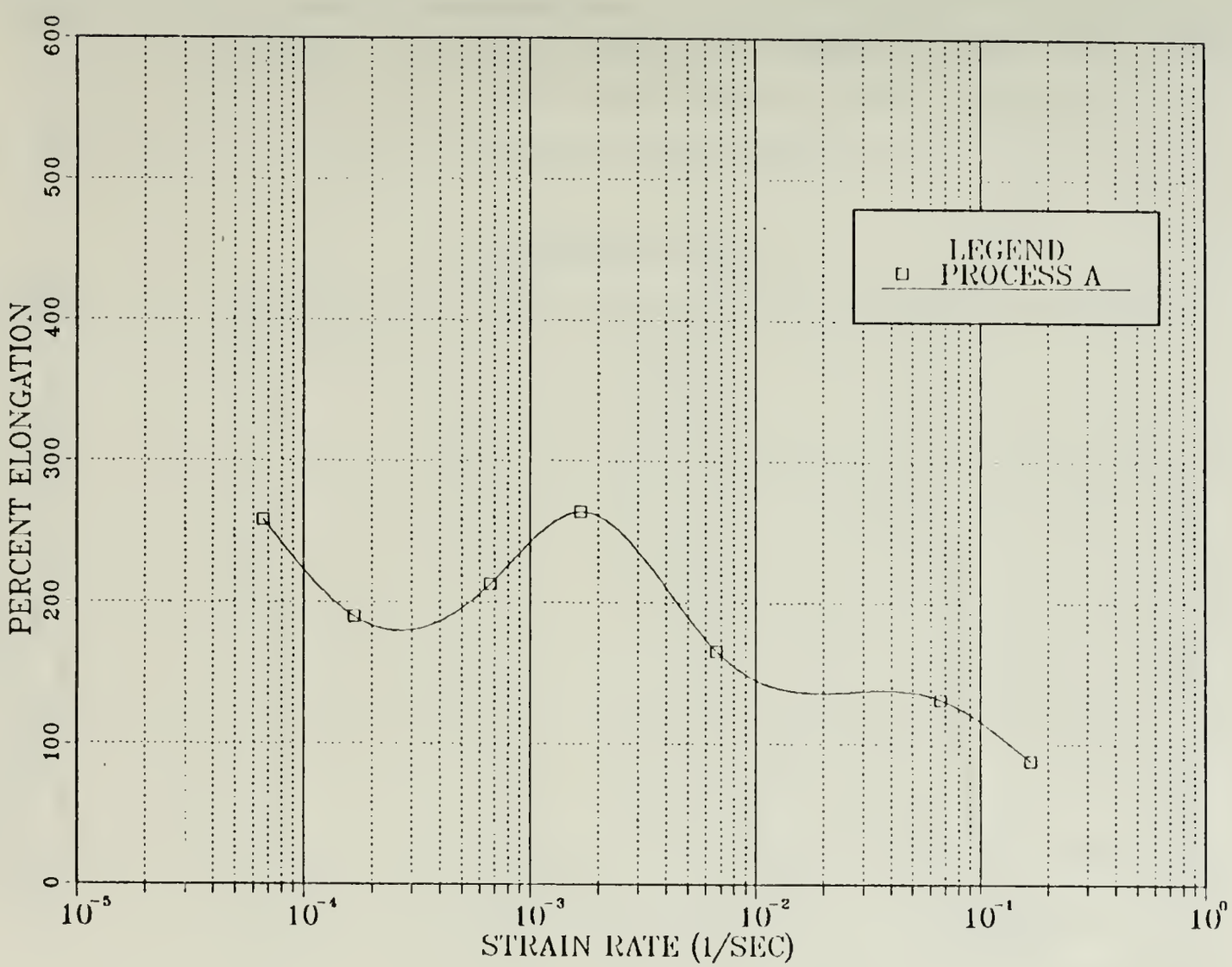

Figure A.7 Ductility vs. strain rate for the Al-10Mg-0.1Zr alloy, tension tested at 300°C with strain rates varying from 6.67×10^{-5}(1/sec) to 1.67×10^{-1}(1/sec). Material was warm rolled at 300°C to a total nominal strain of 2.5 using process A.

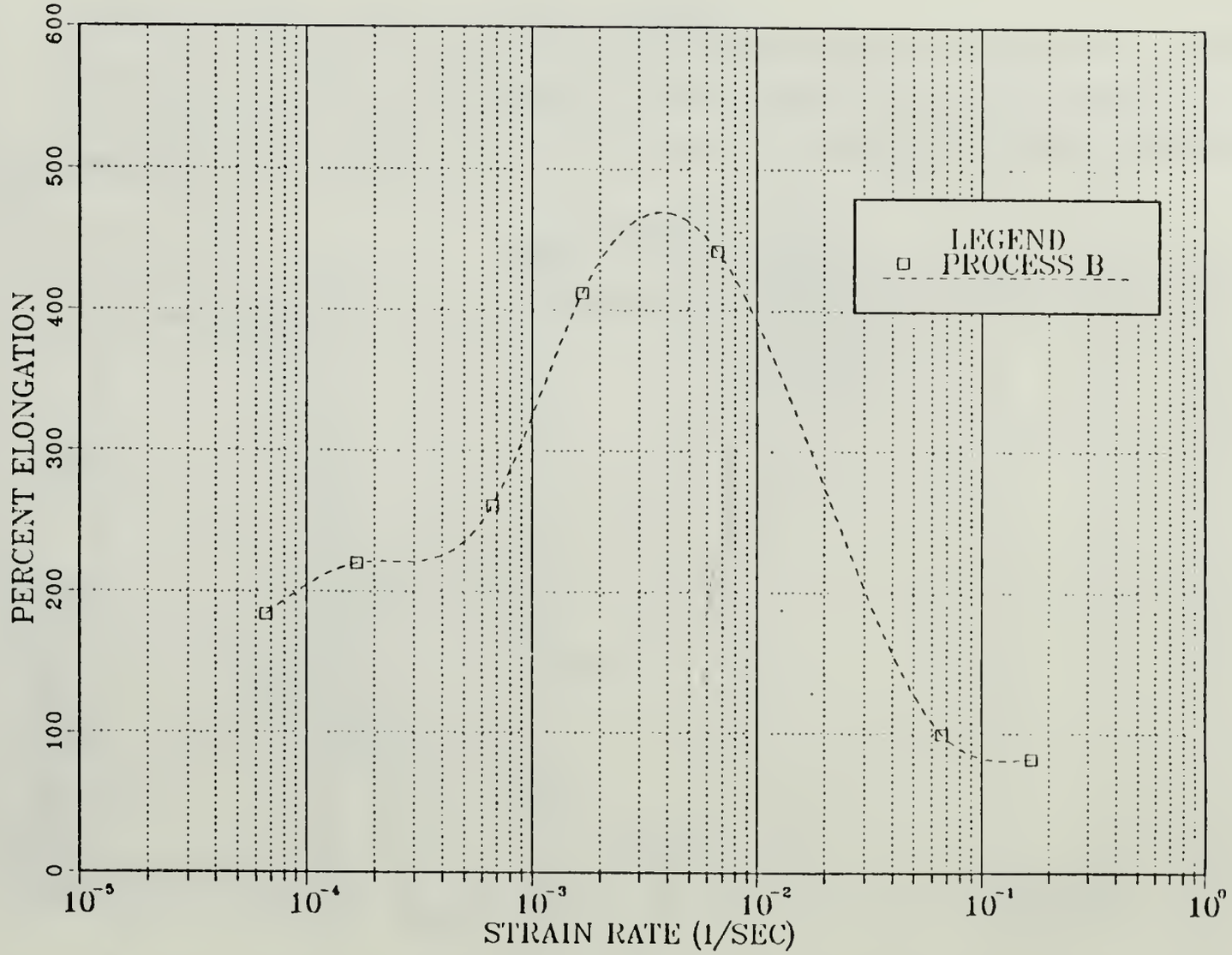

Figure A.8 Ductility vs. strain rate for the Al-10Mg-0.1Zr alloy, tension tested at 300°C with strain rates varying from 6.67×10^{-5}(1/sec) to 1.67×10^{-1}(1/sec). Material was warm rolled at 300°C to a total nominal strain of 2.5 using process B.

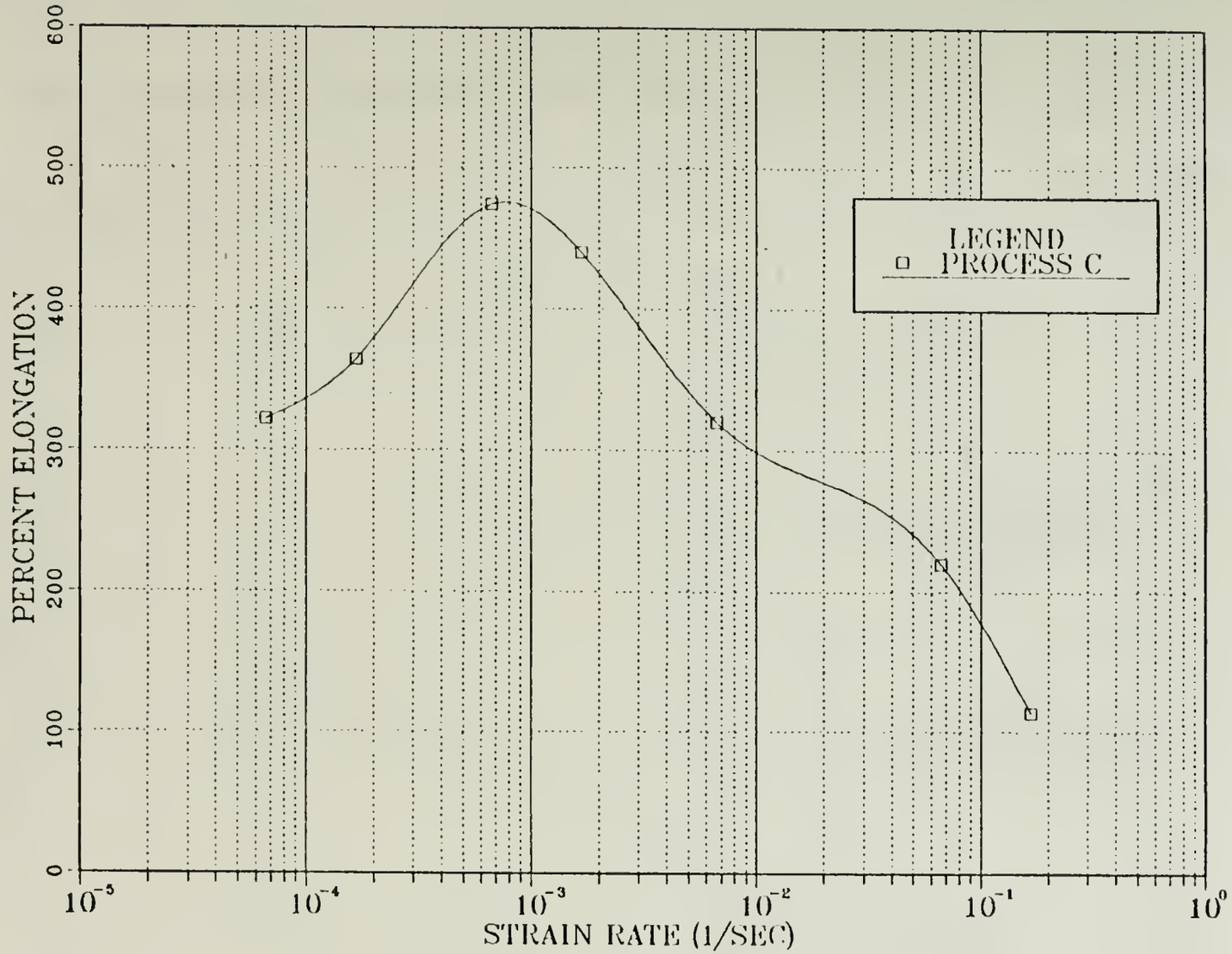

Figure A.9 Ductility vs. strain rate for the al-10Mg-0.1Zr alloy, tension tested at 300°C with strain rates varying from 6.67×10^{-5}(1/sec) to 1.67×10^{-1}(1/sec). Material was warm rolled at 300°C to a total nominal strain of 2.5 using process C.

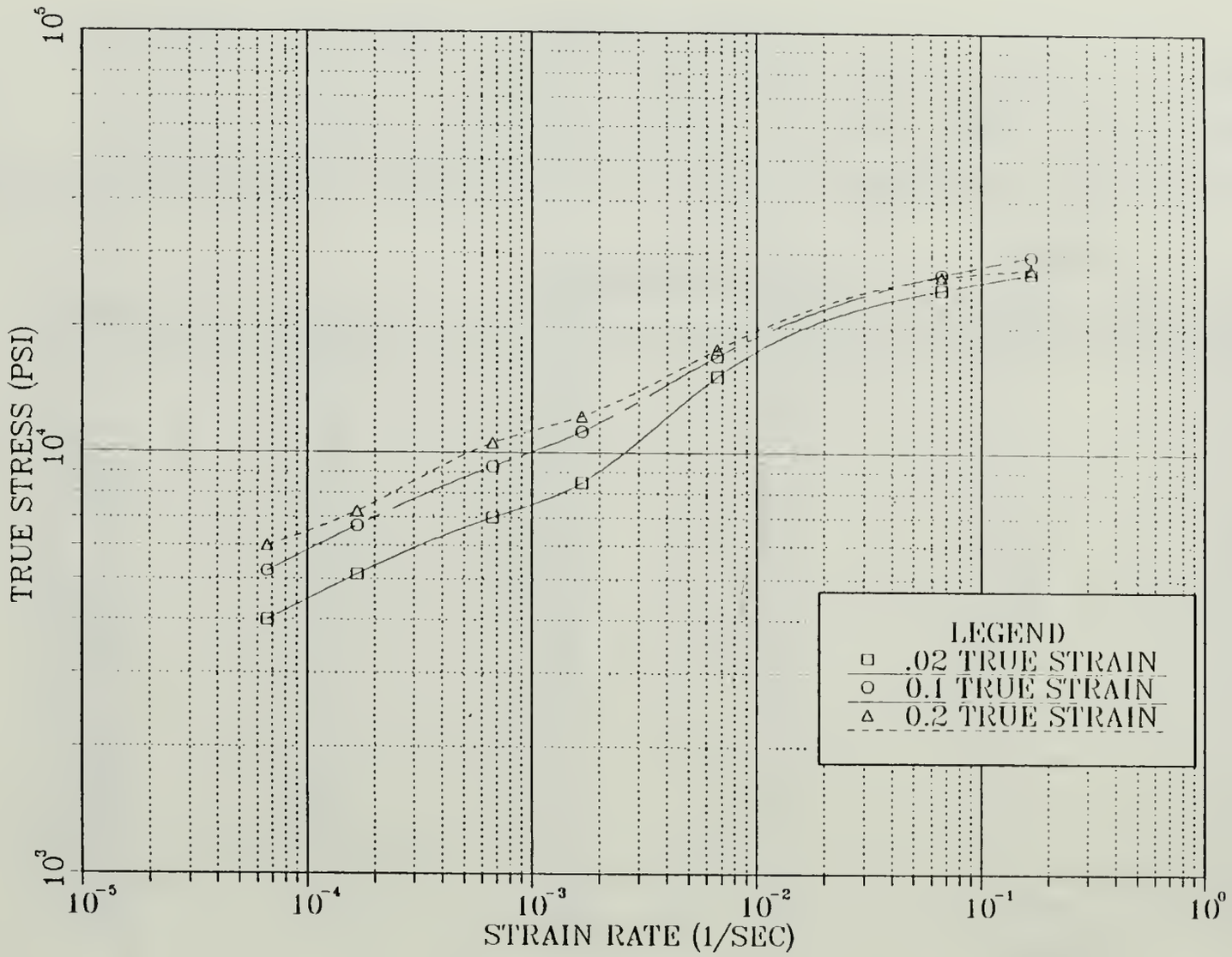

Figure A.10 True stress at 0.02, 0.1 and 0.2 strain vs. strain rate for Al-10Mg-0.1Zr alloy, tension tested at 300°C with strain rates varying from 6.67×10^{-5}(1/sec) to 1.67×10^{-1}(1/sec). Material was warm rolled at 300°C to a total nominal strain of 1.5 using process D.

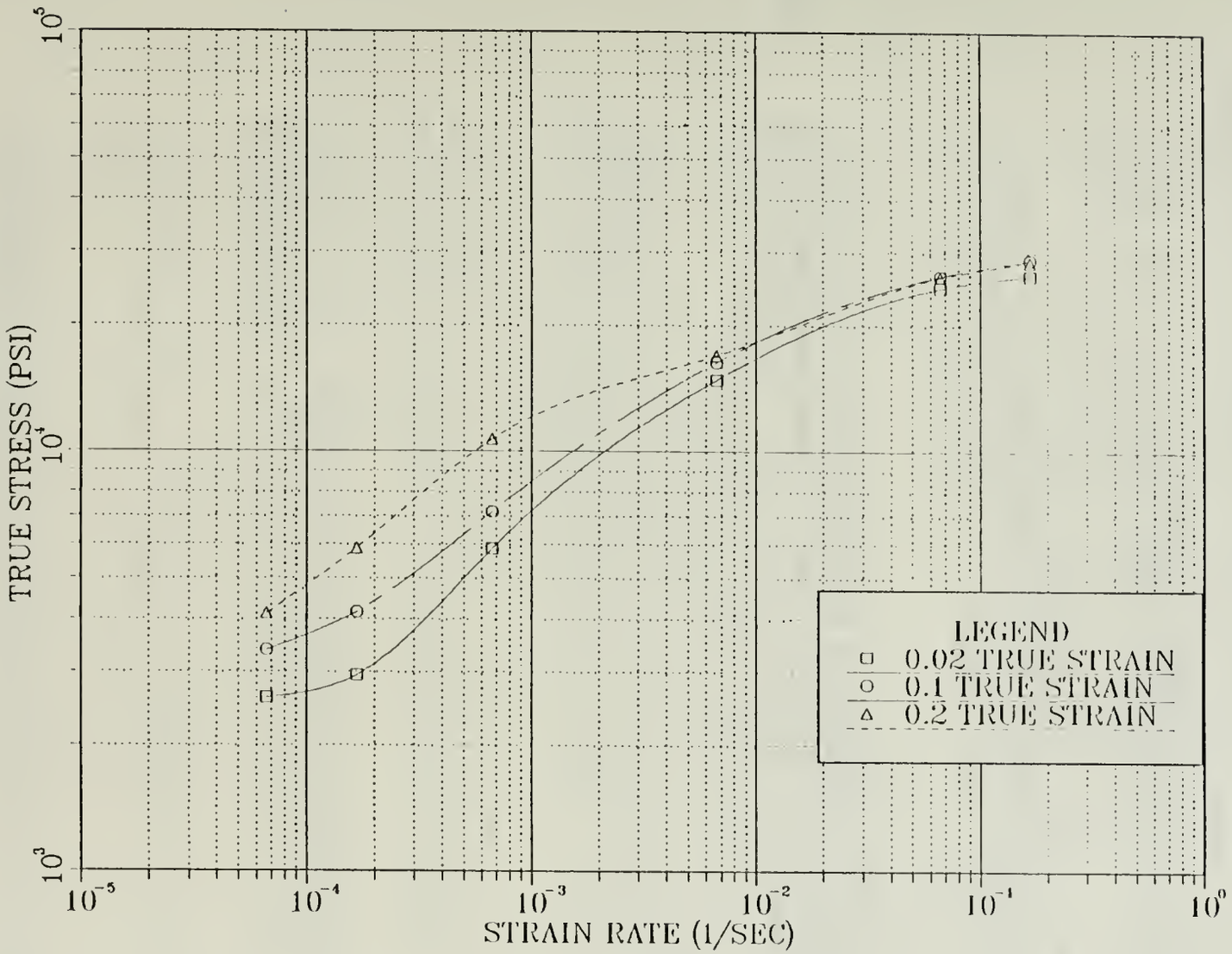

Figure A.11 True stress at 0.02, 0.1 and 0.2 strain vs. strain rate for Al-10Mg-0.1Zr alloy, tension tested at 300°C with strain rates varying from 6.67×10^{-5}(1/sec) to 1.67×10^{-1}(1/sec). Material was warm rolled at 300°C to a total nominal strain of 1.5 using process E.

APPENDIX B

COMPUTER PROGRAM

```
10   INPUT "WHAT FILENAME.<FT> DO YOU WISH TO USE ";D$
20   INPUT "SAMPLE ID..",ID$
30   INPUT "SCALE FACTOR..",SCALE
40   INPUT 'CROSSECTIONAL AREA CU.  IN..",AO
50   INPUT "MAGNIFICATION RATIO..",MAG
60   OPEN "O",#1,D$
70   INPUT "ENTER THE LOAD,LBF..",F
80   INPUT "ENTER X MEASURE FROM CHART,IN..",DELX
90   S=F/AO
100  DEL=(DELX*SCALE)/MAG
110  E=DELL/0.5
120  BIGMA=S*(1+E)
130  EPSLION=LOG(1+E)
140  WRITE #1,F,DELX,S,E,SIGMA,EPSILON
150  INPUT "HIT RETURN TO CONT.,N NEW SPECIMEN, OR Q..",ANS$
160  IF ANS$="" GOTO 70
170  IF ANS$="N" THEN CLOSE #1:CLS:GOTO 10
180  IF ANS$="Q" THEN CLOSE #1:GOTO 190
190  END
```

LIST OF REFERENCES

1. Hertzberg, R.W., Deformation and Fracture Mechanics of Engineering Materials 2nd Ed., John Wiley and Sons, 1983.

2. Berthold, D.B., Effects of Temperature and Strain Rate on the Microstructure of a Deformed, Superplastic Al-10%Mg-0.1%Zr Alloy, M.S. Thesis, Naval Postgraduate School, Monterey, California, June 1985.

3. Grider, W.J., The Effect of Thermomechanical Processing Variables on Ductility of a High-Mg, Al-Mg-Zr Alloy, M.S. Thesis, Naval Postgraduate School, Monterey, California, June 1986.

4. Johnson, R.B., The Influence of Alloy Composition and Thermomechanical Processing Procedure on Microstructural and Mechanical Properties of High-Magnesium Aluminum Alloys, M.S. Thesis, Naval Postgraduate School, Monterey, California, June 1980.

5. Shirah, R.H., The Influence of Solution Time and Quench Rate on the Microstructure and Mechanical Properties of High Magnesium Aluminum-Magnesium Alloys, M.S. Thesis, Naval Postgraduate School, Monterey, California, December 1981.

6. McNelley, T.R. and Garg, A., "Development of Structure and Mechanical Properties in Al-10.2 Mg by Thermomechanical Processing," Scripta Metallurgical, Vol. 18, pp. 917-920, 1984.

7. Alcamo, M.E., Effect of Strain and Strain Rate of Microstructure of a Superplastically Deformed Al-10%Mg-0.1%Zr Alloy, Mechanical Engineer Thesis, Naval Postgraduate School, Monterey, California, June 1985.

8. Underwood, L.F., "A Review of Superplasticity and Related Phenomena," Journal of Metals, pp. 914-919, 1962.

9. Stengall, M.J., "Cavitation in Superplasticity," Superplastic Forming of Structure Alloys, Conference Proceedings of TMS-AIME, pp. 321-336, June 1982.

10. Hart, E.W., "Theory of the Tensile Test," Acta Metallurgica, Volume 15, pp. 351-355, 1967.

11. Nabarro, F.R.M., Report of a Conference on the Strength of Solids, Physical Society (Publishers), London, p. 75, 1948.

12. Herring, C., "Diffusional Viscosity of A Polycrystalline Solid," Journal Applied Physics, Volume 21, p. 437, 1950.

13. Coble, R.L., "A Model for Boundary Diffusion Controlled Creep in Polycrystalline Materials," Journal Applied Physics, Volume 34, p. 1679, 1963.

14. Ashby, M.F., "A First Report on Deformation-Mechanism Maps," Acta Metallurgica, Volume 20, p. 887, 1972.

15. Hartmann, T.S., Mechanical Characteristics of a Superplastic Aluminum-10%Mg-0.1%Zr Alloy, M.S. Thesis, Naval Postgraduate School, Monterey, California, June 1985.

16. Ashby, M.F. and Verrall, R.A., "Diffusion-Accomodated Flow and Superplasticity," Acta Metallurgica, Vol. 21, pp. 149-163, 1973.

17. Sherby, O.D. and Wadsworth, J., "Development and Characterization of Fine-Grain Superplastic Materials," Deformation, Processing, and Structure, pp. 354-384, 1982.

18. Klankowski, K.A., Retained Ambient Temperature Properties of Superplastically Deformed Al-10%Mg-0.1Zr, Al-10%Mg-0.5%Mn and Al-10%Mg-0.4%Cu Alloys, M.S. Thesis, Naval Postgraduate School, Monterey, California, December 1985.

19. Williams, J.C. and Starke, E.A., "The Role of Thermomechanical Processing in Tailoring the Properties of Aluminum and Titanium Alloys," Deformation, Processing, and Structure, edited by G. Krauss, American Society of Metals, Metals Park, Ohio, pp. 279-354, 1984.

20. McQueen, H.J., Journal of Metals, Vol. 32, pp. 17-26, 1980.

21. McQueen, H.J., Chia, E.H., and Starke, E.A., Journal of Metals, Vol. 38, pp. 19-24, 1986.

22. Scott, T.E., "Ingot and Billet Processing of Aluminum Alloys," Aluminum Alloys Their Physical and Mechanical Properties, Volume III, pp. 1406-1407, 1986.

23. Alcoa Technical Center, Ltr, August 1984.

24. Becker, J.J., Superplasticity in Thermomechanically Processed High-Magnesium Aluminum Magnesium Alloys, M.S. Thesis, Naval Postgraduate School, Monterey, California, March 1984.

25. Oster, S.B., Effect of Thermomechanical Processing on the Elevated Temperature Behavior of Lithium-Containing High Mg, Al-Mg Alloys, M.S. Thesis, Naval Postgraduate School, Monterey, California, June 1986.

26. Lee, E.W. and McNelley, T.R., "Microstructure Evolution During Processing and Superplastic Flow in a High Mg, Al-Mg Alloy," in press, Material Science and Engineering.

27. Solomos, D., The Effect of Processing and Superplastic Deformation on Ambient Ductility of Al-Mg-Zr Alloy, M.S. Thesis, Naval Postgraduate School, Monterey, California, March 1987.

INITIAL DISTRIBUTION LIST

		No. of Copies
1.	Defense Technical Information Center Cameron Station Alexandria, Virginia 22304-6145	2
2.	Library, Code 0142 Naval Postgraduate School Monterey, California 93943-5002	2
3.	Department Chairman, Code 69Hy Department of Mechanical Engineering Naval Postgraduate School Monterey, California 93943-5000	1
4.	Professor T.R. McNelley, Code 69Mc Department of Mechanical Engineering Naval Postgraduate School Monterey, California 93943-5000	5
5.	Dr. Steve J. Hales, Code 69He Department of Mechanical Engineering Naval Postgraduate School Monterey, California 93943-5000	1
6.	Dr. Lewis E. Slater, Code AIR 931A Headquarters, Naval Air Systems Command Washington, D.C. 20361	1
7.	Jeff Waldman Naval Air Development Center Materials Science Department Warminster, Pennsylvania 18974	1
8.	Dr. Eu Whee Lee Naval Air Development Center Materials Science Department Warminster, Pennsylvania 18974	1
9.	LT James E. Wise II, USN 251 Levis Drive Mt. Holly, New Jersey 08060	4

Thesis
W65255
c.1

Wise
The influence of total strain, strain rate and reheating time during warm rolling on the superplastic ductility of an Al-Mg-Zr alloy.